

---

Theses and Dissertations

---

Fall 2014

# Design, fabrication and analysis of thermal storage solar cooker prototype for use in Rajasthan, India

Matthew Damon Mercer  
*University of Iowa*

Copyright 2014 Matthew Damon Mercer

This thesis is available at Iowa Research Online: <http://ir.uiowa.edu/etd/1486>

---

## Recommended Citation

Mercer, Matthew Damon. "Design, fabrication and analysis of thermal storage solar cooker prototype for use in Rajasthan, India." MS (Master of Science) thesis, University of Iowa, 2014.  
<http://ir.uiowa.edu/etd/1486>.

---

Follow this and additional works at: <http://ir.uiowa.edu/etd>

 Part of the [Mechanical Engineering Commons](#)

DESIGN, FABRICATION AND ANALYSIS OF THERMAL STORAGE  
SOLAR COOKER PROTOTYPE FOR USE IN RAJASTHAN, INDIA

by

Matthew Damon Mercer

A thesis submitted in partial fulfillment of the requirements for the Master of  
Science degree in Mechanical Engineering in the Graduate College of  
The University of Iowa

December 2014

Thesis Supervisor: Professor H.S. Udaykumar

Graduate College  
The University of Iowa  
Iowa City, Iowa

CERTIFICATE OF APPROVAL

---

MASTER'S THESIS

---

This is to certify that the Master's thesis of

Matthew Damon Mercer

has been approved by the Examining Committee for the thesis requirement for the  
Master of Science degree in Mechanical Engineering at the December 2014 graduation.

Thesis Committee:

---

H.S. Udaykumar, Thesis Supervisor

---

Hongtao Ding

---

James Buchholz

## ACKNOWLEDGEMENTS

The work outlined in this thesis would not have been possible without the contributions of many people. I would first like to express how appreciative I am to Uday for giving me the opportunity to continue my education at the University of Iowa and for getting me involved in such an interesting research area. I have learned and accomplished more as a student than I ever thought possible, because of him. Also, I'd like to thank my friend and colleague Seth Dillard for always teaching me something when we talked. I was always learning from him, even when his point would get lost between cheesy impressions and movie quotes that I often didn't understand.

I am very thankful to all of the people who helped with the creation of my design: Brandon Barquist at IIHR, Steve Struckman and my friends in the engineering machine shop and also Curt Fountain and the guys at the Facilities Management machine shop. I want to extend my thanks for their patience and support during the fabrication process.

Finally, I am forever grateful to my family, especially my parents, Damon and Cheryl Mercer, for their love and support. Any success of mine is a reflection of their hard work. I am extremely fortunate to have them in my life.

## ABSTRACT

Sustainable energy solutions are necessary in developing nations as current food preparation practices are becoming harmful to the environment, economic development and the overall health of the population.

The purpose of this study was to create a Scheffler reflector-based solar cooker prototype, experimentally analyze the system and predict its behavior when subjected to the solar conditions of Rajasthan, India. Former designs from India, the University of Iowa and several other institutions were consulted during the formulation of the prototype design. While referring to a specific set of design constraints, pertinent to developing countries, a Scheffler reflector and tracking stand were fabricated. Solutions for a thermal storage unit were investigated for eventual integration with the prototype.

Solar flux data for Iowa and India was used to predict the amount of energy transmitted by the reflector. Experiments were designed and completed to observe the temperatures experienced at the focal point of the reflector and estimate the energy stored by a steel mass. A series of sun angles, monthly solar flux data and experimental data were used to predict the performance of the storage unit, over a three day span, in Rajasthan. Aspects of the system were then modified to investigate their effects on the temperature of the storage unit.

## PUBLIC ABSTRACT

Solar cooking practices are needed in developing countries as the use of firewood causes health hazards and is destructive to the environment. Simple solar cookers are often disregarded in these areas because of various cultural and technological limitations that affect where and when the cooking is done as well as how solar energy is collected and stored. The goal of this study was to create and analyze a solar cooker prototype according to design constraints pertinent to Rajasthan, India.

The effectiveness of several solar collection and thermal storage methods were investigated in order to produce a new design. Experiments were completed to observe how much energy was being relayed from the sun to a thermal storage unit. Monthly solar energy data was compared with experimental data and used to predict the behavior of the solar cooker when subjected to the sun conditions in Rajasthan. Furthermore, aspects of the design were modified to investigate their influence on the performance of the thermal storage unit.

## TABLE OF CONTENTS

LIST OF TABLES	vi
LIST OF FIGURES	vii
CHAPTER	
1. INTRODUCTION	1
1.1. Problem Introduction	1
1.2. Design Constraints	3
1.3. Previous Cooker Designs	4
1.4. Past University of Iowa Designs	5
1.5. Current State of Research and Development	7
1.6. Design Goals and Strategy	11
2. CHOOSING THE SCHEFFLER DISH	12
2.1. Benefits of Scheffler Dish	12
2.2. Modeling the Scheffler Dish	13
2.3. Computer Modeling of Dish	15
2.4. Manufacturing Dish	19
3. DESIGN OF STORAGE UNIT	20
3.1. Previous Storage Unit Designs	20
3.2. Computer Simulations	20
3.3. Solar Salts and Aluminum	24
4. DESIGN OF TRACKING SYSTEM	28
4.1. Scheffler Dish Tracking	28
4.2. Design and Fabrication of Tracking System	29
5. ANALYSIS	33
5.1. Energy Transmitted by Dish	33
5.2. Testing	38
5.3. Thermal Storage Unit Analysis	43

6.	CONCLUSIONS	49
6.1.	Conclusions	49
6.2.	Recommendations	50
6.3.	Future Work	51
	REFERENCES	53



## LIST OF TABLES

Table 1.1	Population Relying on Biomass	1
Table 4.1	List of Gears and Speeds	32
Table 5.1	Equinox and Solstice Values for $\theta_{\text{eff}}$	35
Table 5.2	Energy Polynomials	37
Table 5.3	Values for Steel Sample Energy Balance	41
Table 5.4	System Energy Constraints	43
Table 5.5	Properties of Latent Heat Phase	44
Table 5.6	Storage Unit Specifications	44

## LIST OF FIGURES

Figure 1.1	Annual Deaths Worldwide by Cause	2
Figure 1.2	Energy Sources for Cooking in India and Botswana	3
Figure 1.3	Namaste Solar Cooker	4
Figure 1.4	Blazing Tube Solar Cooker	5
Figure 1.5	Compound Parabola	5
Figure 1.6	MEDP 2012 Design	6
Figure 1.7	Fresnel Lens	7
Figure 1.8	Wilson Solar Cooker Design	8
Figure 1.9	University of Arizona Fresnel Lens Solar Stove	9
Figure 1.10	Arizona Solar Stove Schematic	10
Figure 1.11	Cal Poly Scheffler Dish	11
Figure 2.1	Section of Scheffler Dish within a Paraboloid	13
Figure 2.2	Scheffler Seasonal Movement	14
Figure 2.3	Average Solar Flux in Cedar Rapids, Iowa	15
Figure 2.4	Average Solar Flux in Jaipur, Rajasthan	16
Figure 2.5	Early Design Orientation	17
Figure 2.6	Small Model of Scheffler Dish	18
Figure 2.7	Final Scheffler Dish with Dimensional Constraints	18
Figure 2.8	Completed Scheffler Reflector	19

Figure 3.1	Aluminum Model Layout	21
Figure 3.2	Aluminum Surface Temperature	21
Figure 3.3	Enhanced Lithium Nitrate Model	22
Figure 3.4	Enhanced Lithium Nitrate Surface Temperature	23
Figure 3.5	Solar Salt Thermal Storage Unit	24
Figure 3.6	Preliminary Solar Battery Testing	25
Figure 3.7	Heating of Solar Salt Battery with Fresnel Lens	26
Figure 4.1	Positioning of Scheffler Dish	28
Figure 4.2	Position of Rotational Axis	29
Figure 4.3	Preliminary Tracking System Design	30
Figure 4.4	Gear and Pendulum System	30
Figure 4.5	Final Sprocket Orientation	31
Figure 4.6	Completed Tracking Stand	32
Figure 5.1	Dish Rotation vs. Ideal Design	34
Figure 5.2	Solar Energy Flux for Iowa and India	36
Figure 5.3	Monthly Iowa Energy Curves	37
Figure 5.4	Monthly India Energy Curves	38
Figure 5.5	Experimental Set-up	39
Figure 5.6	Heating and Cooling of Steel Sample	40
Figure 5.7	Heating of Second Steel Sample	42
Figure 5.8	Thermal Storage Unit Temperature Response	45

Figure 5.9	Storage Unit Temperature by Reflector Area	47
Figure 5.10	Storage Unit Temperature by Mass of Solar Salts	47
Figure 6.1	Low Heat Solar Salt Temperature Distribution	51
Figure 6.2	Overall Storage Unit Temperature Distribution	52

CHAPTER 1  
INTRODUCTION

**1.1 Problem Introduction**

As industrialized nations search for more sophisticated sustainable energy solutions there still exist many societies that rely on primitive forms of energy to survive. More than 2.5 billion people in developing countries depend on wood, charcoal, agricultural waste and animal dung as energy sources for cooking. When viewed as “living off the land” these practices appear harmless, however, when resources are harvested unsustainably and energy conservation technologies are inefficient, there are serious adverse consequences for health, the environment and economic development [1].

Table 1.1: Population Relying on Biomass [1]

	<u>Total population</u>		<u>Rural</u>		<u>Urban</u>	
	%	million	%	million	%	million
Sub-Saharan Africa	76	575	93	413	58	162
North Africa	3	4	6	4	0.2	0.2
India	69	740	87	663	25	77
China	37	480	55	428	10	52
Indonesia	72	156	95	110	45	46
Rest of Asia	65	489	93	455	35	92
Brazil	13	23	53	16	5	8
Rest of Latin America	23	60	62	59	9	25
<b>Total</b>	<b>52</b>	<b>2 528</b>	<b>83</b>	<b>2 147</b>	<b>23</b>	<b>461</b>

The world health organization (WHO) estimates that 1.5 million premature deaths per year are directly attributable to indoor air pollution from the use of solid fuels. That is more than 4000 deaths per day with over half of them children under five years of age. More than 85% of these deaths (about 1.3 million people) are attributable to biomass use, and the rest is due to the use of coal [1]. Figure 1.1 shows the comparison of deaths from biomass pollution to some other leading world-wide killers.

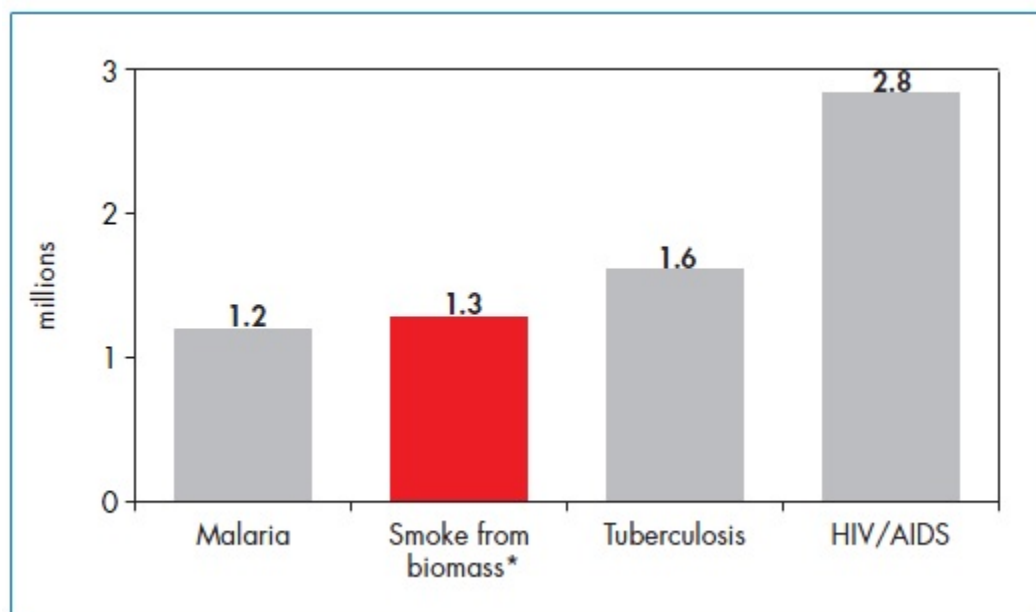


Figure 1.1: Annual Deaths Worldwide by Cause [1]

India is a country in which substantial amounts of wood is harvested for fuel, as illustrated in Figure 1.2. Rajasthan, the country's largest state, has experienced significant deforestation leading to the expansion of the bordering Thar Desert. Unless considerable reduction in fire wood usage is seen in the near future, the livability of the region will come into question.

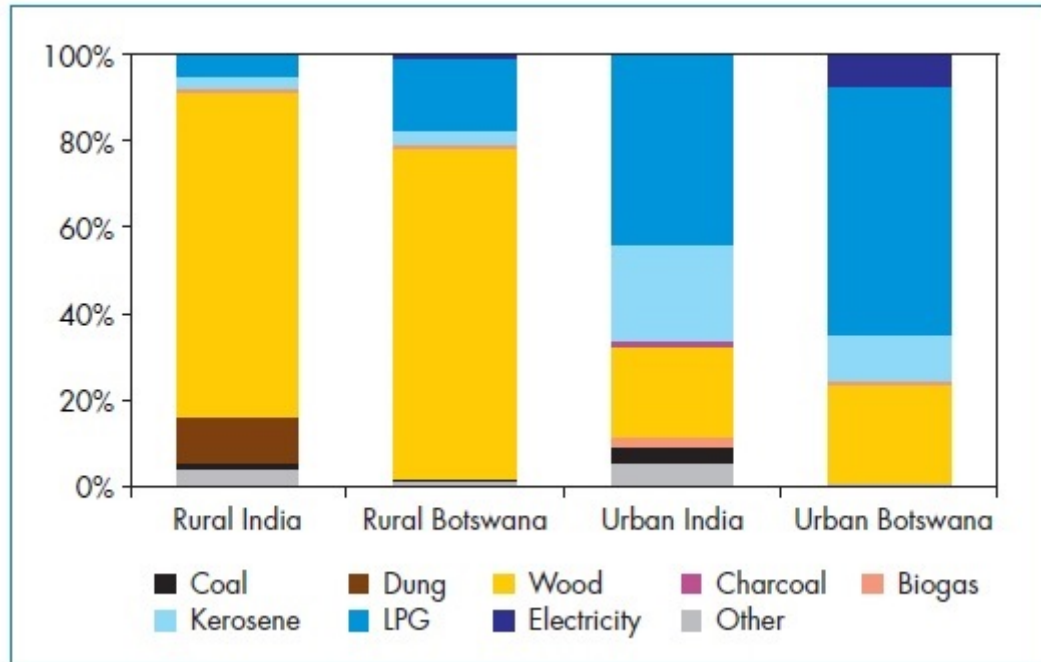


Figure 1.2: Energy Sources for Cooking in India and Botswana [1]

With an average insolation of  $5.5 \text{ kWh/m}^2$  per day, the solar energy in Rajasthan is abundant. However, due to the technological limitations in the rural sectors, this energy is vastly underutilized. Given the abundance of sunshine, the diminishing regional biomass resources, and the problems inherent to indoor cooking with biofuels, a successful implementation of solar cookers in Rajasthan could prove life changing with far-reaching implications throughout India and the rest of the world.

## 1.2 Design Constraints

The developing regions of Rajasthan provide not only technological but cultural constraints, which often overlap, and create a small window in which to design. The only pure technical constraint, and most challenging overall, is the lack of electricity in the rural villages of Rajasthan. Due to the lack of access to funding and outside resources, the

components would need to be manufactured locally and at a low cost.

The habitual tendencies of the villagers provide more detailed criteria to design around. First, the cooking is done in the early morning and late evening, in the absence of sunshine. Thus, a thermal storage device or “solar battery” must be incorporated with the design. Next, cooking times could range up to two hours per meal so a substantial amount of energy would need to be stored throughout the day. The most energy-intensive part of the meal is roti, which requires temperatures between 200 and 250 °C supplied over a duration of 2 hours. Thus, an estimated 4 kWh would need to be stored each day to supply enough heat for morning and evening cooking. Also, the cooking is done inside, demanding the battery be stationary. Lastly, the system will be operated and maintained by the citizens of the village requiring the mechanics of the design to be robust and easily repaired.

### 1.3 Previous Cooker Designs

There have been attempts in recent years to integrate low cost solar cookers into



Figure 1.3: Namaste Solar Cooker

rural Indian communities, but the designs have generally found limited success due to robustness issues or lack of thermal storage capabilities. The Namaste Solar Cooker was a parabolic design made up of two petals coated in reflective Mylar that focused on an elevated cooking dish (Figure 1.3). The design produced enough energy to cook, however, the heat around the dish was so



intense that the villagers could not properly handle the food. Over time, the Mylar coating on the petals began to tear and delaminate, demanding that improved robustness be investigated for future designs. Additionally, the design could not be used after sunset, as there was no storage unit, and needed to be manually adjusted throughout the day to maintain the position of the focal spot.

The Blazing Tube Solar Cooker, shown in Figure 1.4, was another design aimed



Figure 1.4: Blazing Tube Solar Cooker

at incorporating thermal storage. The design consisted of a reflective trough focused on a tube filled with oil, creating a thermosiphon in which heated oil ran into a tank at the end of a trough with cooler oil circulated back into the tube. The oil, while conductive, lost heat rapidly once it was in the tank resulting in poor energy storage.

#### 1.4 Past University of Iowa Designs

There have been developments at the University of Iowa on solar cookers for use in Rajasthan over previous years. Starting in the spring of 2011, in the Mechanical Engineering Design Project course (MEDP), these designs integrated a compound parabola solar collector to focus the sunlight. The parabola was designed to remain stationary throughout the day, creating a focal line with intensity that varies depending on



Figure 1.5: Compound Parabola

the position of the sun (Figure 1.5).

The first design used a collector, made from polished aluminum, to focus on a storage unit filled with sand and insulated with rice hulls. It was found that the polished aluminum was not reflective enough to relay a sufficient amount of light and that the sand had a thermal conductivity that was too low to absorb and store the energy. Also, the weight of the storage unit exceeded five hundred pounds making it difficult to move.

In the fall of the same year some adjustments were made in an attempt to continue making improvements to the design. The same class, with new students used a Mylar coating on the parabola in an attempt to reflect more light and aluminum was mixed with the sand to improve the storage unit's thermal conductivity. It was found that the Mylar would need to be replaced with a more reflective material and that a large amount of aluminum still needed to be added to the storage unit.

A new approach was taken in the spring of 2012. One set of students attempted to completely revamp the compound parabola system while another group created a Scheffler dish, a reflective dish that focuses the light to a small focal spot. The parabola was lined with acrylic mirrors in place of the Mylar that was previously applied, in an effort to improve reflectivity and durability. The design was further altered to focus the sun's light on a pipe system containing oil rather than directly into the thermal storage medium. The heated oil flowed upward into a small storage unit containing sand and aluminum. Within the storage unit was a heat pipe with a protruding

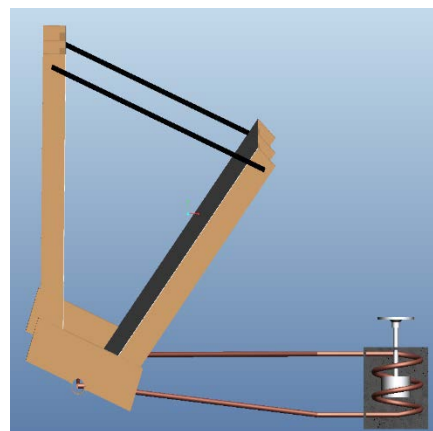


Figure 1.6: MEDP 2012 Design

surface used for cooking (Figure 1.6). A Scheffler reflector was successfully constructed using aluminum framing, Velcro and acrylic mirrors.

The developments, once again, found limited success. The compound parabola system was inefficient because of the many media with which the solar energy was interacting. While the Scheffler dish was a step in the right direction, the focal spot was too large due to inaccuracies in the shape of the aluminum framing.

In 2013 a Fresnel lens was analyzed to determine its potential relevancy to the

system. A Fresnel lens is basically a flat magnifying glass; a convex lens concentrically collapsed onto a plane, resulting in ridges that preserve the curvature and focal length of the original lens shape (Figure 1.7). While the Fresnel lens produces a small and

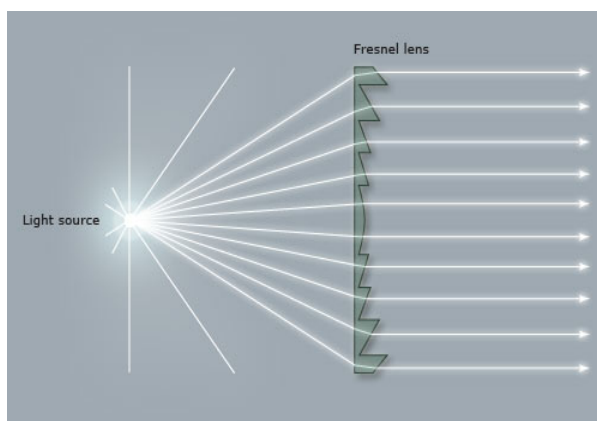


Figure 1.7: Fresnel Lens

accurate focal point, it is difficult to find a lens large enough to satisfy the system's energy needs.

### **1.5: Current State of Research and Development**

Research involving solar cooking in the developing world has been compiled at the University of Arizona, California Polytechnic State University and MIT. With similar efforts across the country, and in such respected departments, awareness on this issue is constantly increasing.

In 2006, work was done at MIT on the Wilson solar cooker, named after Professor

David Gordon Wilson. A Wilson solar cooker was designed to be used under conditions with little or no insulation. The temperatures within the storage unit would reach levels as high as 258 °C. The proposed heat-storage material was lithium nitrate, a substance shown to hold the required temperatures for up to 6 hours and temperatures above 100 °C for up to 25 hours. It was expected that a meal for six people could be prepared up to 6 hours after charging of the thermal battery [2]. As of 2006 a prototype had not yet been fabricated, only designed. A schematic of the design is shown in Figure 1.8.

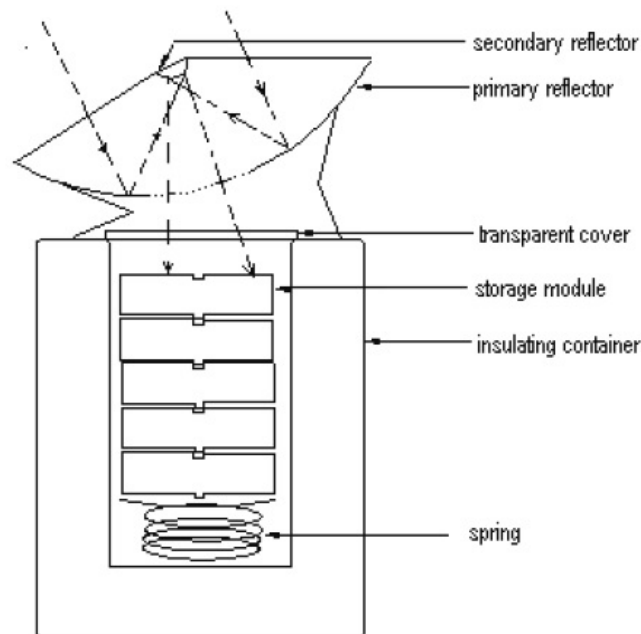


Figure 1.8: Wilson Solar Cooker Design [2]

The studies performed on the proposed design show that it would satisfy many of the design constraints listed earlier. The major downside to the design is the cost of the lithium nitrate. In order to store 13 MJ, approximately 3.6 kWh, the design would require 78.6 pounds of lithium nitrate, costing nearing \$700. The literature does not provide a total cost for the entire device but accounting for material and manufacturing

cost, along with the lithium nitrate, the feasibility of this design flourishing in a developing nation is uncertain.

Students at the University of Arizona fabricated a solar cooking stove using a Fresnel lens in 2009. The goal of the design was to demonstrate high safety and efficiency of solar cooking and heating using Fresnel lenses, resources that are low in cost and readily available. The design consisted of a stove with a fixed heat-receiving area located at the focal point of the lens. A tracking system was used to rotate the lens about the focal point in both zenith and azimuth angles. The maximum temperatures experienced at the stove were as high as 300 °C [3]. The design is pictured in Figure 1.9, below.

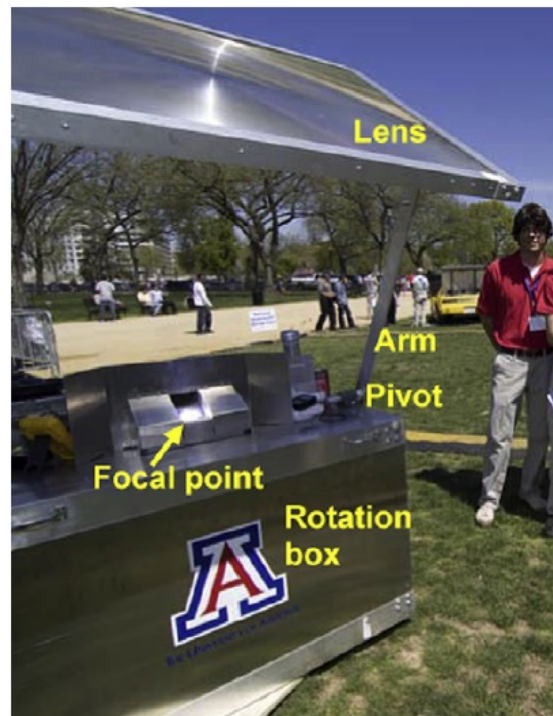


Figure 1.9: University of Arizona Fresnel Lens Solar Stove [3]

The students at Arizona were successful in creating a functional, sophisticated and aesthetically pleasing design. It includes a feature using mineral oil that allows the user to cook outside or inside (Figure 1.10).

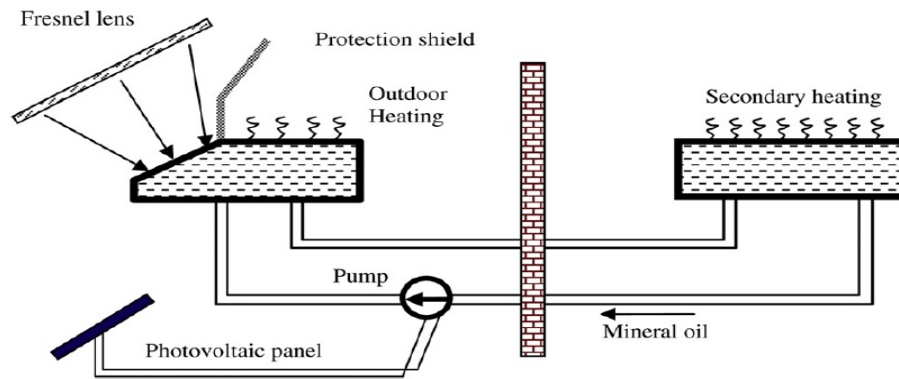


Figure 1.10: Arizona Solar Stove Schematic [3]

However, it was found that the mineral oil in the system is the limiting factor. It was assumed that the outdoor surface temperature could go higher if the system was not restricted by the maximum allowable temperature of the mineral oil [3]. Other drawbacks of this design include manual adjustment tracking and lack of a thermal storage unit.

The Scheffler reflector and thermal storage design of Cal Poly is similar to the work being done at Iowa. A Scheffler dish was constructed using aluminum and Lexan for the frame as well as reflective aluminum and mirror material for the surface (Figure 1.11). A thermal storage unit and tracking system were theorized but have not been constructed. The proposed storage unit would comprise of concrete with pumice as insulation while the tracking system would be a combination of electronic and mechanical components. Some preliminary testing was done with the dish and peak temperatures of 375 °C were reached [4].

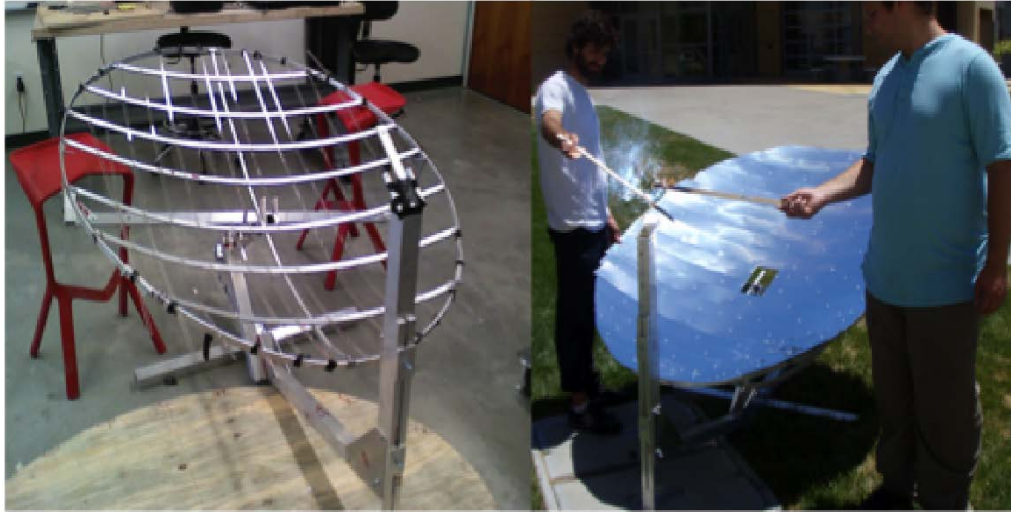


Figure 1.11: Cal Poly Scheffler Dish [4]

### 1.6: Design Goals and Strategy

With knowledge of past failures and successes involving solar cookers, a goal was set to fabricate a fully functional Scheffler dish with a tracking system while working within the constraints listed in Section 1.2.

The first step to completing this goal was to design a reflector that optimized the miniaturization of the focal point. A computer model of the dish would be produced and milled to ensure acceptable accuracy. Next, a support stand and gear system, with no electrical components, would be fabricated to allow the dish to rotate opposite the earth, keeping the focal point fixed throughout the day. Concurrently, a thermal storage unit, doubling as a cooking surface, would be utilized to house the energy transmitted from the dish. Finally, experiments would be implemented to examine peak temperatures, energy stored and overall efficiency of the system.

## CHAPTER 2

### THE SCHEFFLER DISH

#### **2.1: Benefits of Scheffler Dish**

From the developments made in the University of Iowa MEDP class in 2012 it was determined that the Scheffler reflector was the proper light focusing apparatus to be used in future designs. That decision was reached for a variety of reasons.

Inconsistencies and size constraints were the reasons for moving away from the Fresnel lens and compound parabola. As stated earlier, a Fresnel lens large enough to meet the energy criteria does not exist and would be costly to manufacture.

Though it can remain stationary while tracking the sun, the compound parabola creates a focal line that varies in intensity throughout the day, i.e., as the sun rises a hot spot develops at one end of the focus and moves to the other end as the earth rotates. Because of the length of the focus and movement of the hot spot, the compound parabola requires a storage unit with a sizeable collection area.

The Scheffler dish can effectively eliminate large surfaces on the thermal storage unit. Theoretically, a solar battery with a top surface area of  $3 \text{ m}^2$ , left in the sun, would absorb as much energy, if not more, than a  $3 \text{ m}^2$  Scheffler dish could relay to a small battery. However, because the large surface would be uninsulated, convective losses would be much higher than those of a small storage unit.

The small focal point of a Scheffler dish allows for a significant reduction in the thermal storage collection area. Use of a small thermal storage unit creates flexibility in the overall design of the system. Not only does it preserve the comfortable cooking



environment but also presents the possibility of a mobile storage unit.

The most convenient upside to a well-designed Scheffler reflector is that it can track the sun's movement, relative to earth, throughout the day, along a single axis. This involves the fabrication of a support stand that allows the system to stay stationary at all times. Although some occasional maintenance would be required on the system, it is able to traverse during the day with little supervision.

## 2.2: Modeling the Scheffler Dish

The Scheffler design is no more than a lateral section of a paraboloid, a three dimensional bowl-shaped geometry that reflects light to a single point (Figure 2.1) [5].

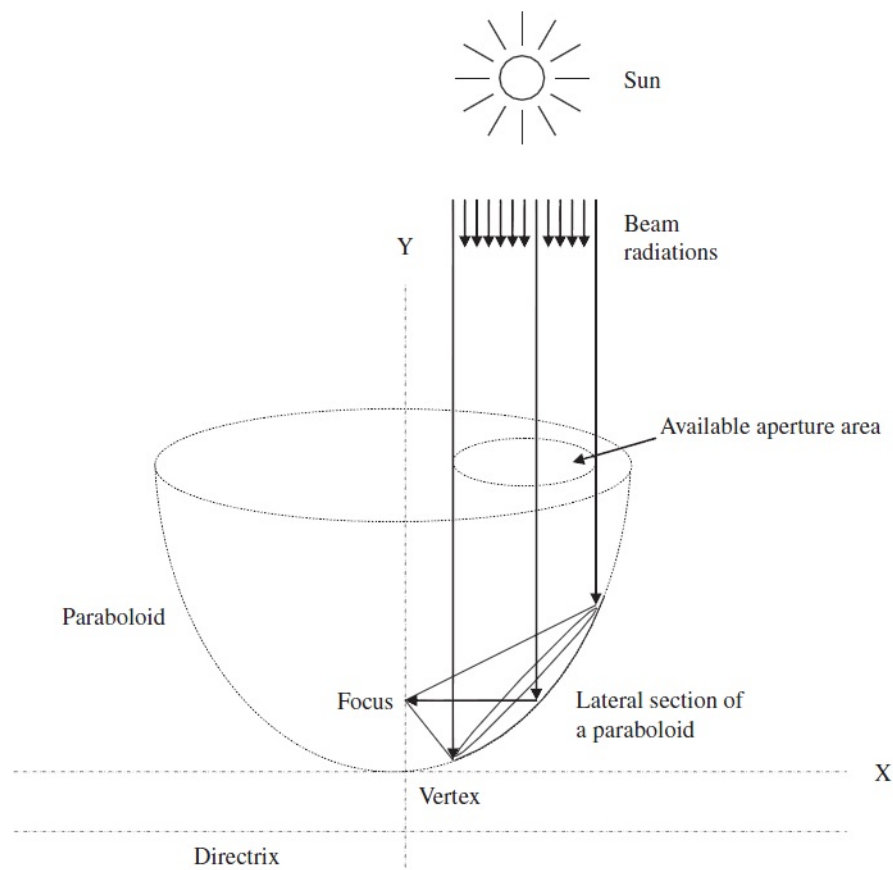


Figure 2.1: Section of Scheffler Dish within a Paraboloid [5]

This shape can also be represented as a parabola, most commonly described by the equation  $y = x^2$ , revolved around the y-axis. The focus of the parabola with equation  $y = ax^2 + bx + c$ , always lies on the y-axis and its length ( $f$ ) is characterized by Equation 2.2.

$$f = \frac{1}{(4a)} \quad (2.2)$$

However, due to the earth's orbit and daily rotation, the sun experiences seasonal changes and "moves" in the sky from day to day. Therefore, throughout the year, the y-axis orientation and shape of the parabola need to change to keep the focal point stationary in relation to the center of the dish (Figure 2.2) [6].

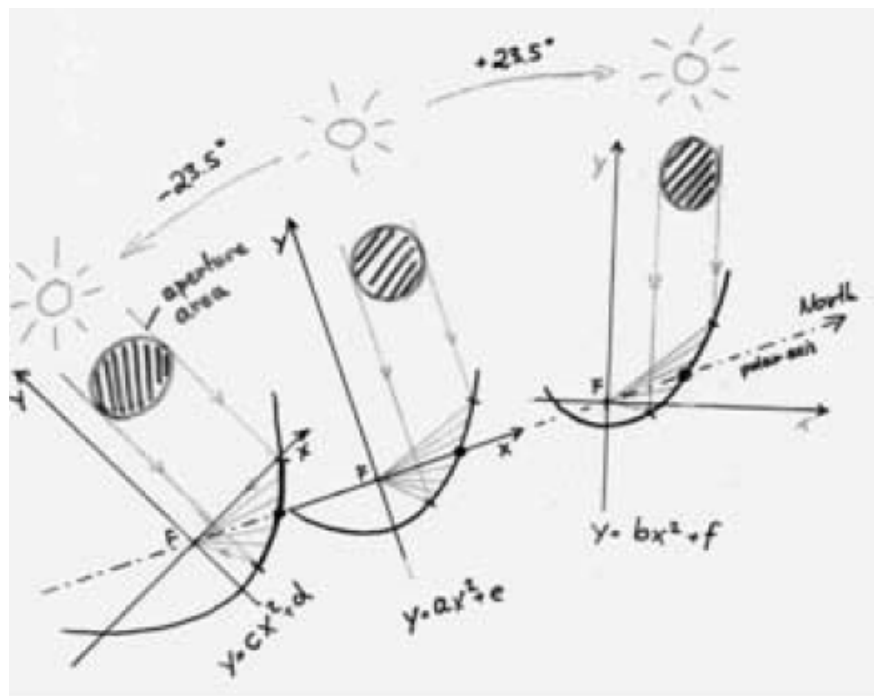


Figure 2.2: Scheffler Seasonal Movement [6]

The constant relationship between the focal point and the center of the dish is important when involving a tracking system which will be discussed in Chapter 4.

### 2.3 Computer Modeling of Dish

Whilst applying constraints to the concepts described in Section 2.2, a Scheffler dish was designed using CAD software. Preliminary limitations were placed on the dish design based on the testing location. First, the dish would be designed to operate in Iowa City, Iowa, for convenient fabrication and transportation. Correspondingly, the solar flux in Iowa is substantially less than that in India. If energy collection goals could be reached in Iowa then, theoretically, they would be more easily reached in Rajasthan.

Unfortunately, Iowa does not experience ample sunshine in the winter months, hence, the decision was made to make the dish operable between the spring and fall equinoxes (April 21 – September 21). Also, the late spring and summer months in Iowa are comparable to the months with the highest solar flux in India, shown in Figures 2.3 and 2.4, respectively. Data provided by the National Renewable Energy Laboratory [7, 8].

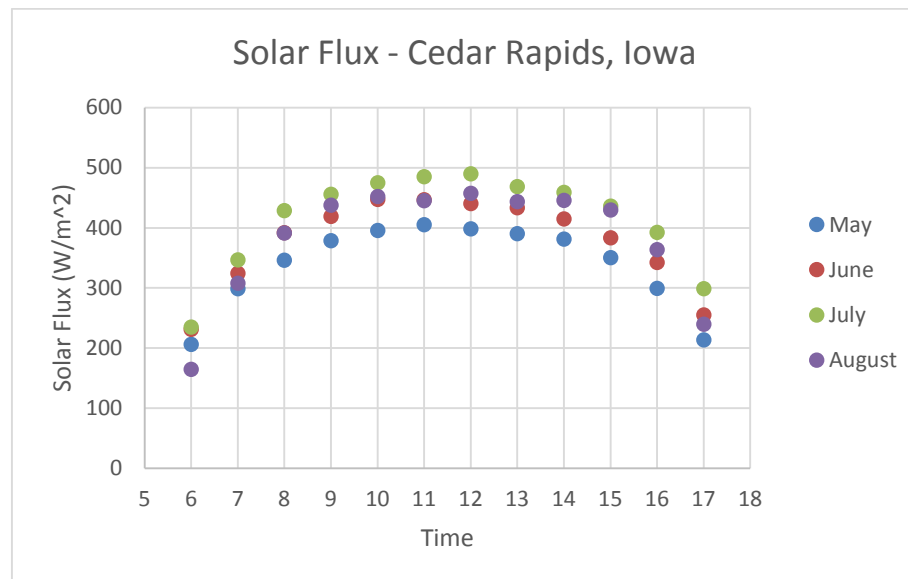


Figure 2.3: Average Solar Flux in Cedar Rapids, Iowa

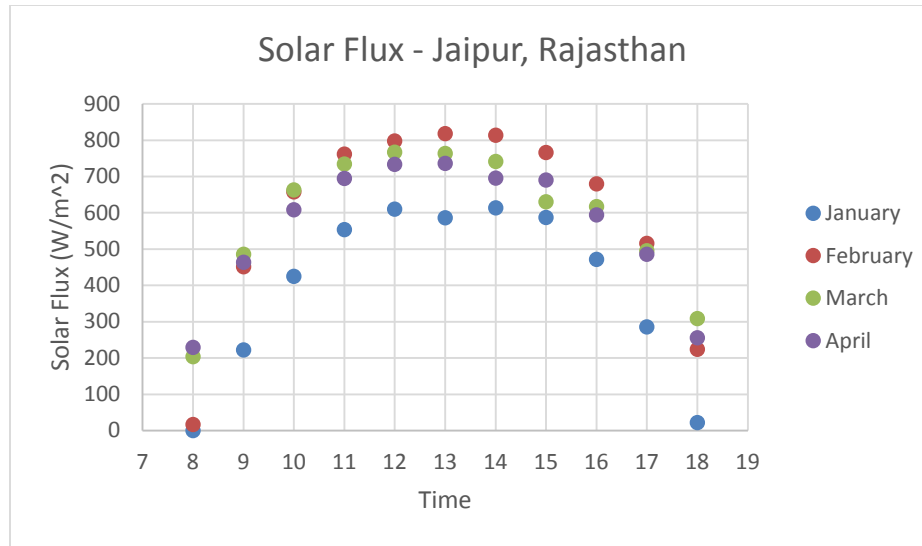


Figure: 2.4: Average Solar Flux in Jaipur, Rajasthan

The latitudinal position of Iowa City is approximately 42 degrees north, indicating the mean sun angle (the sun angle at each equinox) is 48 degrees. As shown in Figure 2.2, in relation to the equinoxes, the sun is 23 degrees higher at the summer solstice (71 degrees) and 23 degrees lower at the winter solstice (25 degrees). Accordingly, the reflector was designed to operate within a 23 degree range with an optimum sun angle of 59.5 degrees (mean of 48 and 71).

Physical dimensions of the dish were needed to further constrain the model. The middle of the dish would lie two feet off the ground and eight feet, diagonally, from the focal point. Also, the dish would be eight feet wide by four feet tall for ease of manufacturing, to be discussed later. The curvature of the dish was then modeled on 3D CAD software. The equation  $y = x^2$ , revolved around the y-axis and having a focal point at (0, 0.25), was used to initiate the curvature. It was then oriented toward the optimum sun angle, 59.5 degrees. This is shown below in Figure 2.5 and resembles the illustration in Figure 2.2.

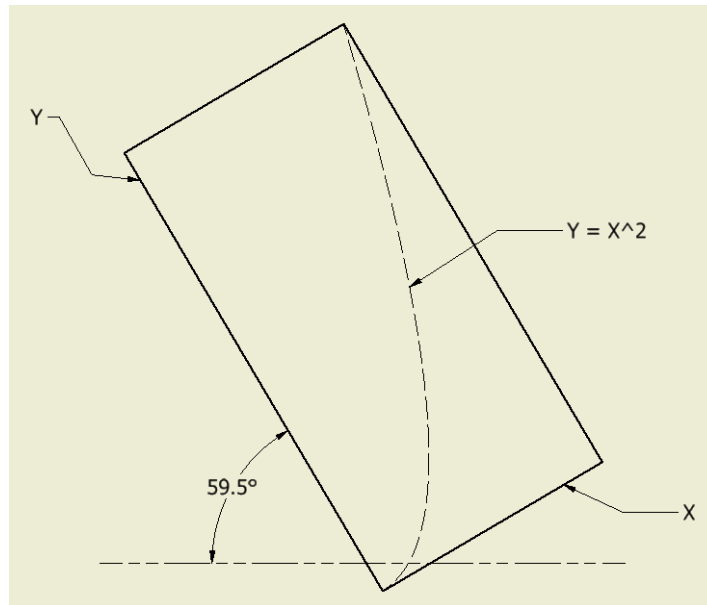


Figure 2.5: Early Design Orientation

With the constraints in relation to the ground and focal point, an angular relationship could be established within the system (Figure 2.6). This relationship was needed to scale the model to actual size (Figure 2.7). It can be observed that the height from ground to focal hypotenuse ratio is consistent between the models at 1:4. The cross section of the dish was designed to be 8 feet wide by 4 feet tall giving it an area of approximately  $32 \text{ ft}^2$ , just under  $3 \text{ m}^2$ . This size was chosen while accounting for ease of manufacturing, to be discussed in the next section.

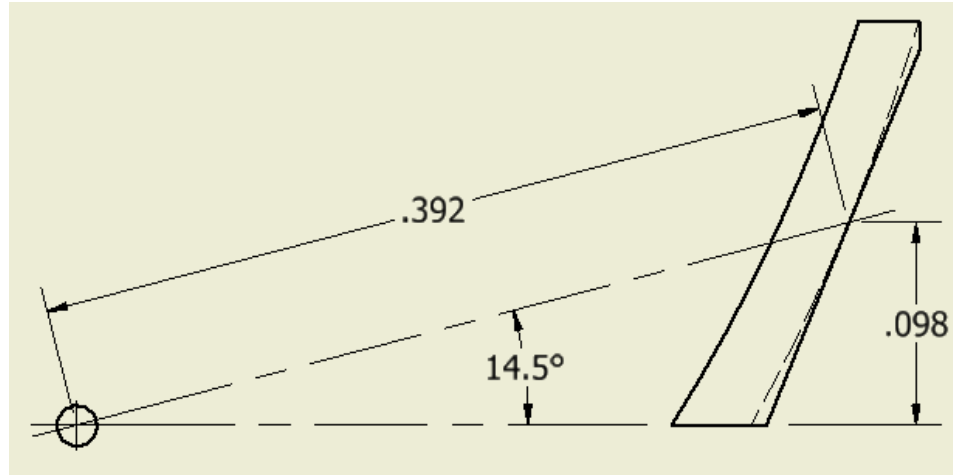


Figure 2.6: Small Model of Scheffler Dish

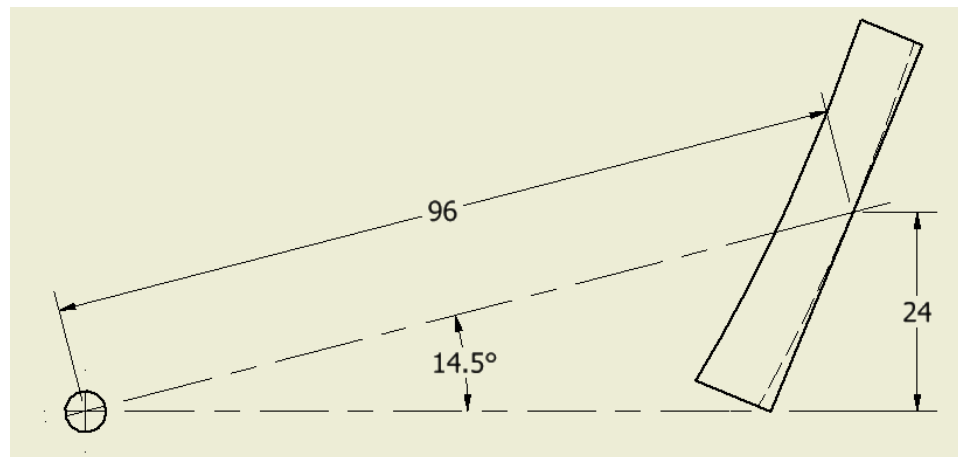


Figure 2.7: Final Scheffler Dish with Dimensional Constraints

#### 2.4: Manufacturing of Dish

A Haas table mill at the Hydraulics Wind Tunnel Annex at the University of Iowa was used to create the final dish shape. Material was removed from a cheap yet durable mass of Styrofoam to form the parabolic curvature. To make the process more effortless, a 4' x 8' x 1' (in depth) chunk of Styrofoam was used and attached to a 4' x 8' sheet of plywood to properly secure it to the table mill.

Given the success of acrylic mirror in past designs it was decided that it was a suitable material with which to coat the dish. A 4' x 8' sheet of mirror was cut into 4' x 3" strips because the full sheet was too rigid to bend in two directions. The strips of mirror were adhered to the Styrofoam using wood glue. The completed Scheffler reflector is shown in Figure 2.8.



Figure 2.8: Completed Scheffler Reflector

## CHAPTER 3

### THERMAL STORAGE UNIT DESIGN

#### **3.1: Previous Storage Unit Designs**

There has been extensive work completed in the development of the thermal energy storage unit in correspondence with the improvements on the light-focusing devices. As mentioned in Chapter 1, students at the University of Iowa first attempted to use sand as the energy storage material. However, the thermal conductivity of sand is too low to absorb the heat. Multiple designs were then constructed using aluminum as an energy transport medium protruding into the sand or mixed with it. Again, though aluminum has a high thermal conductivity and successfully absorbed energy, the sand was still not conductive enough to be effective. To eliminate the use of sand, but still use a material that is cheap and readily available, an attempt was made to use stones as the main thermal storage material. A five gallon steel drum was filled with stones which were then soaked with Duratherm 500 heat transfer oil. It was theorized that the oil would evenly distribute energy throughout the series of stones. However, the oil expanded when heated and had a smoke point below expected temperatures.

Accordingly, more innovative approaches were taken in conceptualizing a solar battery.

#### **3.2: Computer Simulations**

In the spring of 2013, Scott Ruebush, a graduate student at the University of Iowa, began to run computer simulations on potential storage system designs. He first studied a scenario in which a solid block of aluminum was used as the storage material, given its



high thermal conductivity. A system was modeled within ANSYS Fluent, shown in Figure 3.1, of an aluminum cube (square) partially surrounded with rice husk insulation (trapezoid) [9].

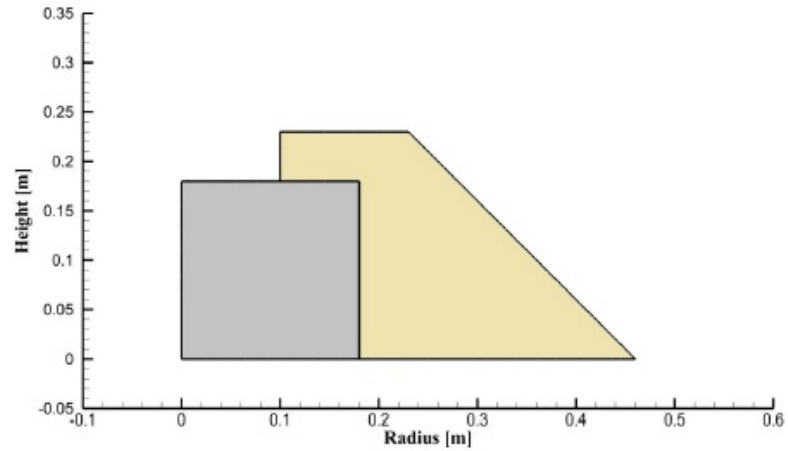


Figure 3.1: Aluminum Model Layout [9]

The system was subject to an energy input of 5 kWh, every day, for one week, between the hours of 9:00 a.m. and 4:30p.m. It can be observed in Figure 3.2, that by the third day, afternoon cooking temperatures were in excess of 400 °C, higher than the preferred cooking temperature range [9].

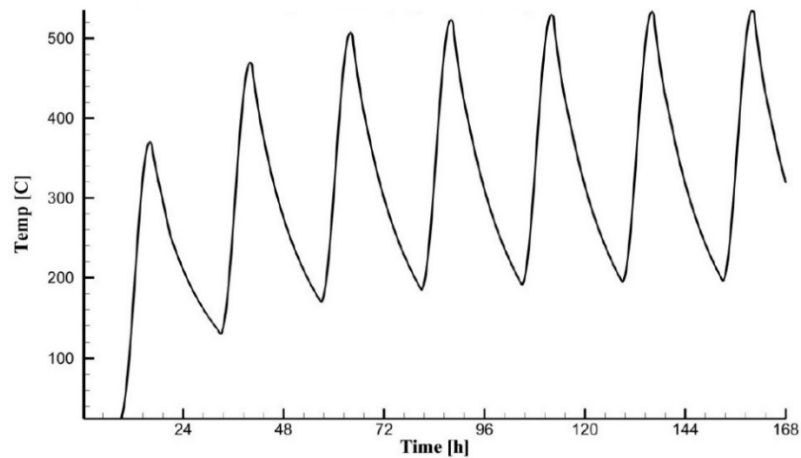


Figure 3.2: Aluminum Surface Temperature [9]

The simulation also showed that morning cooking temperatures would be around 200 °C, which is encouraging. However, a question arises as to whether or not those temperatures could be sustained over a two hour cooking duration.

A series of lithium nitrate and aluminum configurations were studied by Ruebush succeeding the study of solid aluminum. The most successful of these configurations was a block of lithium nitrate filled with aluminum shards and surrounded by an aluminum casing and still partially surrounded by rice husks. The system was assumed to have an effective thermal conductivity of 5.11 W/m\*K. Comparatively, lithium nitrate alone has a thermal conductivity of 0.511 W/m\*K. An illustration of the system is shown in Figure 3.3 [9].

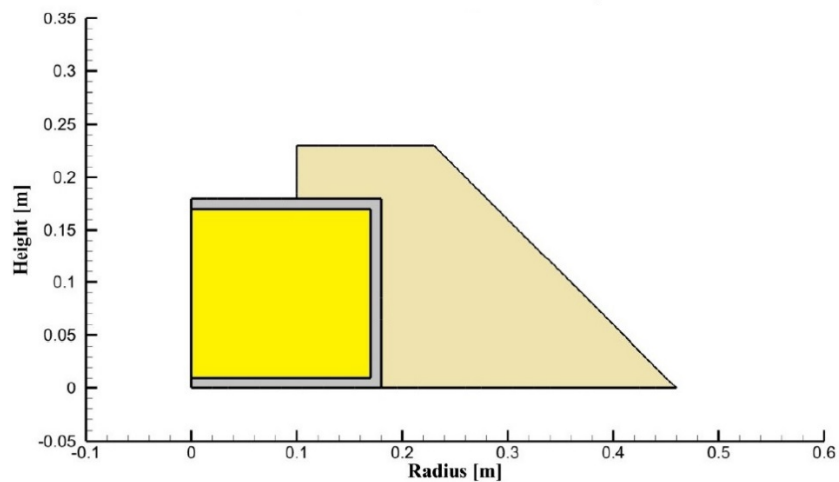


Figure 3.3: Enhanced Lithium Nitrate Model [9]

The same simulation used to evaluate the aluminum block was used for the lithium nitrate system. The lithium nitrate, however, experiences a phase change during heating (solid to liquid) and cooling (liquid to solid) that creates more desirable results. These phase changes can be observed in the temperature data shown in Figure 3.4. During heating,

the spike showing the phase change occurs when the surface temperature is around 390 °C. While the melting point of lithium nitrate is around 260 °C, the material must melt within the unit before its effect is felt at the surface, showing a significant temperature difference between the core and surface. The phase change is again seen in the temperature stabilization when the battery is left to cool. The slow solidification of the lithium nitrate allows the surface to stay relatively stable for an extended period of time, keeping the temperature high enough to use for cooking in the morning [9].

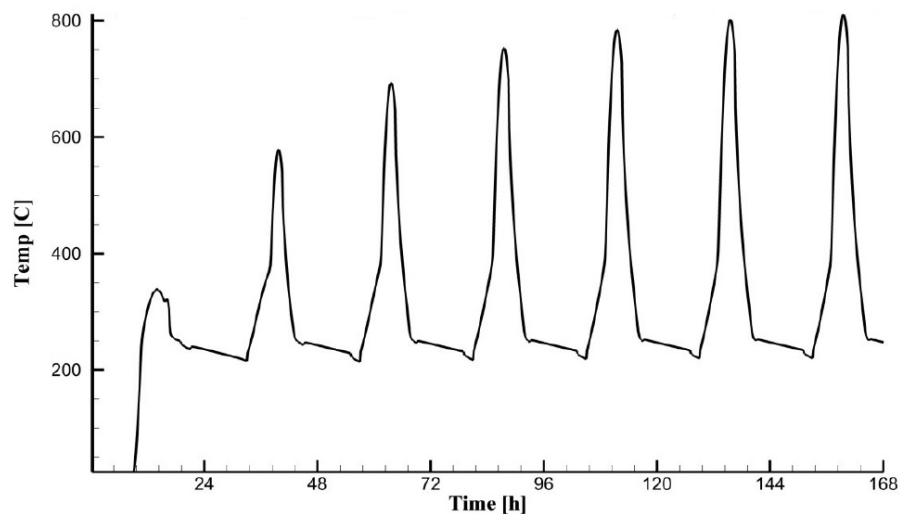


Figure 3.4: Enhanced Lithium Nitrate Surface Temperature [9]

If this model were to be used in practical applications, the afternoon cooking temperatures would still be high. Nevertheless, progress was made in sustaining a morning cooking temperature. Thus, the decision was made to include a phase change material when developing the final thermal storage device.

### 3.3: Solar Salts and Aluminum

In the summer of 2013, Mike Augspurger, a graduate student in mechanical engineering at the University of Iowa began to investigate solutions for a latent heat thermal storage unit, a solar battery that utilizes the steady latent heat of transformation of a material to sustain constant cooking temperatures. His design revolved around the use of “solar salts,” a mixture of sodium nitrate and potassium nitrate. The melting point of these salts is 220 °C, which is easily produced with a reflector or lens of reasonable size, but also within practical cooking temperatures. The salts were housed within a five gallon steel drum along with an aluminum apparatus made up of a core, fins and an exposed top plate. The solar irradiance was to be focused on the top plate and spread to the salts within the drum via the core and fins. An interior box made of concrete board and lined with insulation was used to store the steel drum. Additionally, the interior box was placed within a plywood outer box filled with rice husks [10]. The design configuration is illustrated in Figure 3.5.

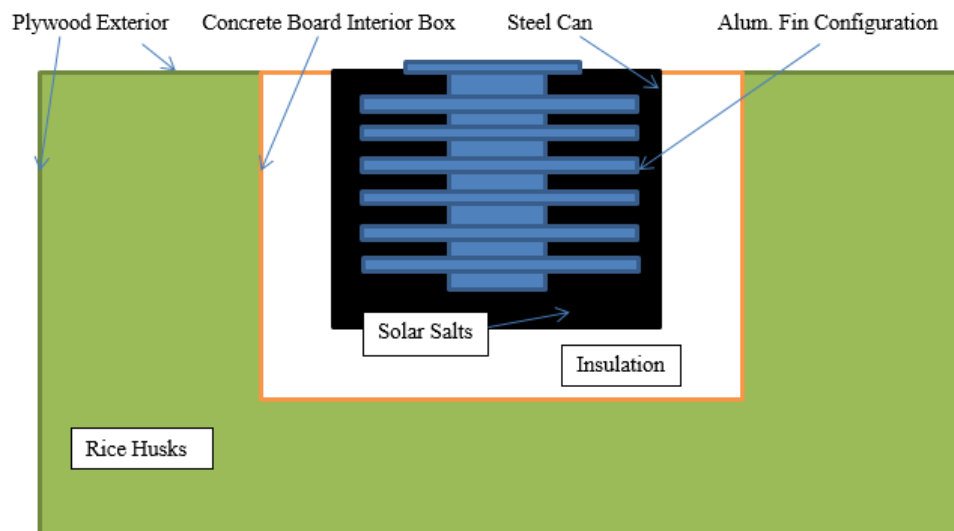


Figure 3.5: Solar Salt Thermal Storage Unit [10]

The properties of the solar salts in this system are similar to the properties of the lithium nitrate used in the simulations by Ruebush, most importantly the thermal conductivity, having a value of approximately  $0.5 \text{ W/m}\cdot\text{K}$ . The aluminum core, having a much higher thermal conductivity, transfers energy to the salts when the system is heated but also takes energy from them when the system cools. It was hypothesized that this storage unit would exhibit behavior similar to the simulations performed by Ruebush but with a stabilization temperature around  $220 \text{ }^\circ\text{C}$ . Experiments were performed on the system using a combination of two Fresnel lenses with areas of  $1.045 \text{ m}^2$  and  $0.621 \text{ m}^2$ : two lenses were used because the larger lens was more opaque than the other, causing it to be less efficient [10]. An illustration of the experimental setup is shown in Figure 3.6.



Figure 3.6: Preliminary Solar Battery Testing [10]

Six thermocouples were affixed to the battery: five to the aluminum, evenly spaced from top to bottom, and one in the salts [10]. Data was collected throughout the day on August 1, 2013 and is shown in Figure 3.7.

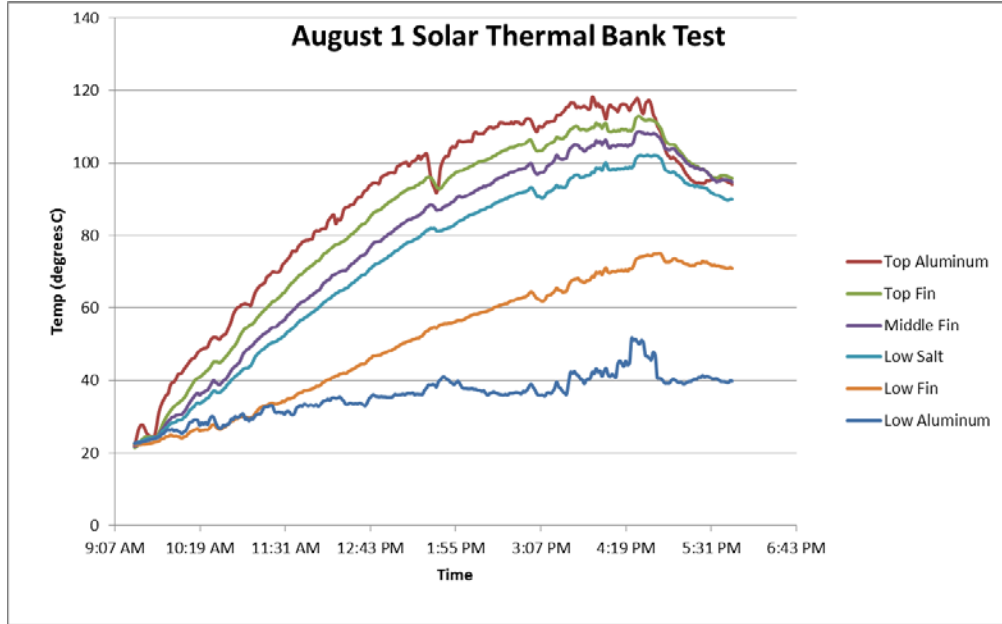


Figure 3.7: Heating of Solar Salt Battery with Fresnel Lenses [10]

As expected, the vertical temperature gradient within the storage unit identifies the hottest temperature at the top, where the light is focused, and the coolest temperature at the bottom due to slow heat transfer through the system. Unfortunately, the highest temperature experienced during the test was approximately 120 °C, well below the salts' melting temperature of 220 °C. An ideal scenario, however, predicts a different outcome. The energy conservation within the system is described by Equation 3.1.

$$mc_p\Delta T = hA\Delta t(T - T_\infty) + \frac{kA_s\Delta t}{L}(T - T_\infty) + Q_{sun}\alpha\cos\theta \quad (3.1)$$

Assuming that the system is perfectly insulated and there are no losses due to conduction in the system, Equation 3.1 reduces to Equation 3.2.

$$mc_p\Delta T = Q_{sun}\alpha\cos\theta \quad (3.2)$$

Also, because the salts and aluminum have similar specific heats, the system will be evaluated as a singular body with constant thermal properties. The aluminum and salt configurations have masses ( $m$ ) of 12.25 kg and 23.5 kg, respectively, for a total of 35.75 kg. The system has an average specific heat ( $c_p$ ) of approximately 0.00025 kWh/kg-C with an ideal absorptivity ( $\alpha$ ) of 1.  $Q_{sun}$  represents the total energy available from the sun during the day. On an average August day in Iowa, the available energy from the sun from 9:30 a.m. to 4:30 p.m. (7 hours), for a 1 m<sup>2</sup> lens, is approximately 4.4 kWh. If the sun is perfectly normal to the lens throughout the day ( $\theta = 0$ ), the change in temperature for the ideal system can be calculated as 492 °C.

This shows that the actual system is experiencing major losses as the real temperature change was about 100 °C. These losses are caused by opaqueness of the lens, absorptivity of the aluminum, inaccuracies of the focal spot, lack of insulation, and occasional cloud cover. While cloud cover will always cause inconsistencies there is still enough solar power, if harnessed efficiently, to reach the desired temperatures within the system. Accordingly, improvements for the system were proposed to improve efficiency. The use of the lens would be abandoned in favor of a Scheffler reflector, the face of the aluminum would be painted with flat black paint capable of withstanding high temperatures and insulation would be added liberally.

CHAPTER 4  
DESIGN OF TRACKING SYSTEM

**4.1: Scheffler Dish Tracking**

There are several factors that prompted the decision to incorporate solar tracking when designing the system. The thermal storage unit must remain stationary for cooking convenience and due to its weight. Additionally, tracking helps to maximize the amount of energy transmitted to the storage unit. Most importantly, a tracking system would significantly reduce the amount of manual labor needed to maintain the entire system. A proficient tracking system would require, at most, two citizens to monitor the position of the focal point, perform occasional maintenance and to reset the system every morning. These tasks would be simple, time-saving and much less physically demanding than collecting firewood on a daily basis.

The design of the tracking system, much like that of the reflector, was focused around Iowa City's latitude.

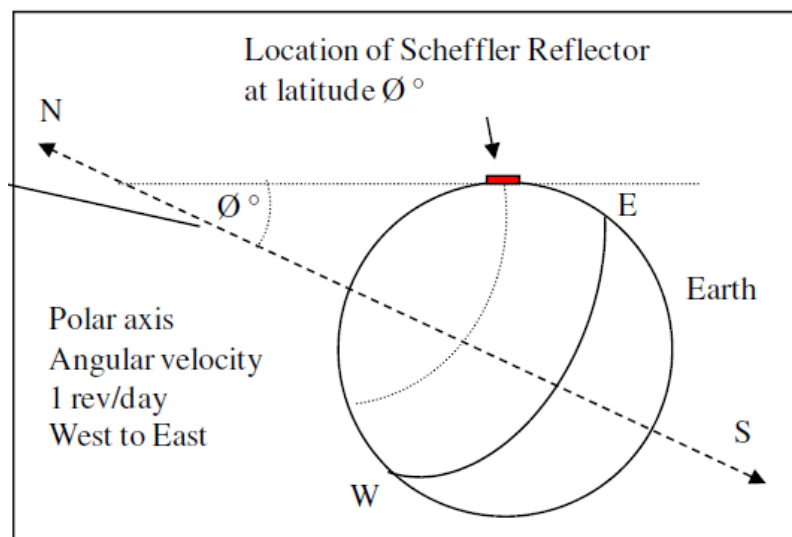


Figure 4.1: Positioning of Scheffler Dish [5]



The rotational axis of the tracking system is parallel to earth's rotational axis and its angle depends on the latitudinal position of the dish (Figure 4.1). Therefore, the rotational axis must be at an angle of 42 degrees from the ground, rotated about the z-axis through the focal point, illustrated in Figure 4.2.

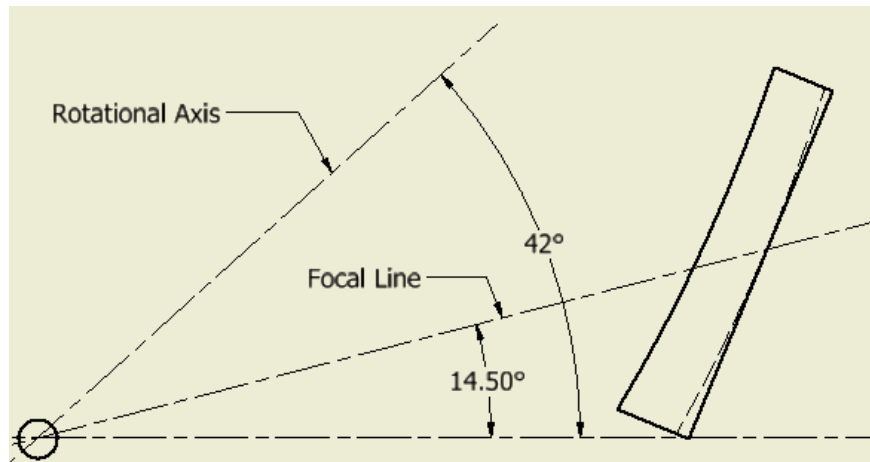


Figure 4.2: Position of Rotational Axis

The design of the tracking system, in its simplest form, was constrained to the dimensional relationship between the rotational axis and the reflector seen above. In theory, the position of the focal point would be conserved throughout the day by moving the dish about the rotational axis.

#### 4.2: Design and Fabrication of Tracking System

The main goals in designing the tracking system were to use materials that are cheap, that can be easily obtained in developing countries, and to practice basic manufacturing techniques that do not require exotic tools or equipment. Some ideas were gathered from previous designs, using a pendulum and counterweight system for power, and a computer model was developed for the tentative prototype (Figure 4.3).

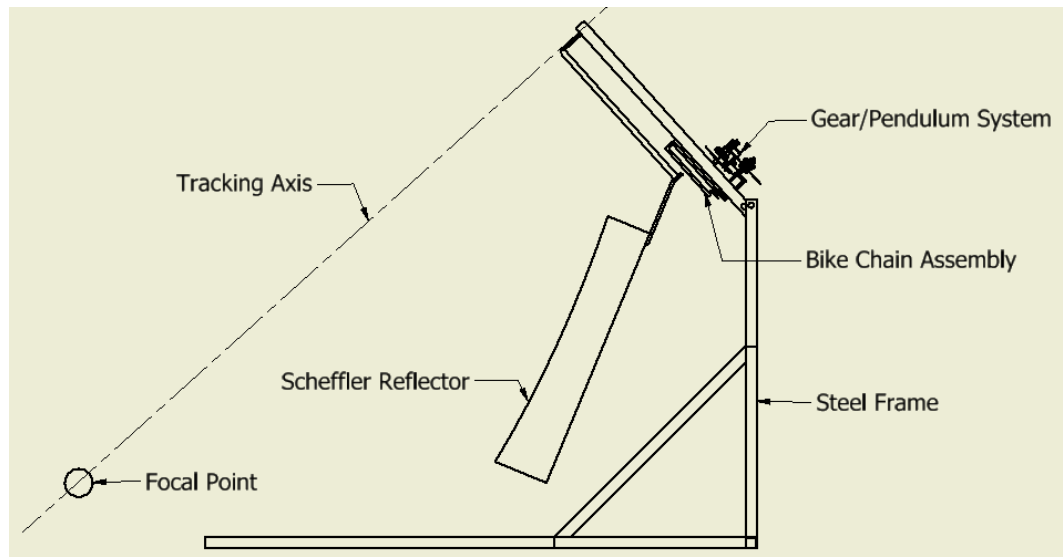


Figure 4.3: Preliminary Tracking System Design

The gear and pendulum system was the first component to be designed and fabricated. An existing design was modified so that it could be properly merged with the designed stand. A computer model was generated and is shown in Figure 4.4.

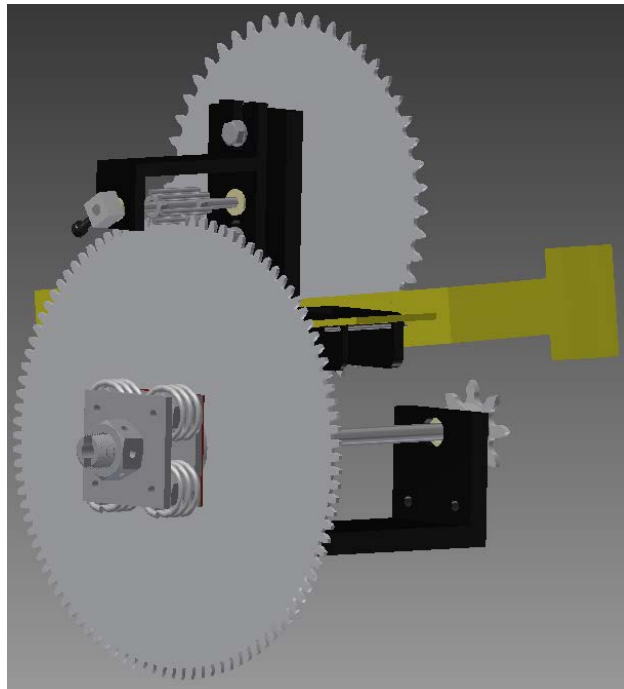


Figure 4.4: Gear and Pendulum System

The design consists of four gears and a spring clutch to account for potential torque on the system. The pendulum would be hooked to a counterweight. Upon initial vertical motion of the counterweight, two pins, attached to the pendulum, would grab the first gear, causing repeated motion of the counterweight. The motion of the counterweight, and subsequent grabbing of pins, would cause the system to repeatedly tick like a clock. The frame and pendulum of the system were fabricated by cutting and welding stock steel, sprockets were either purchased or cut from aluminum, stainless steel shafts were cut and inserted through brass sleeves and standard nuts and bolts were used for various purposes.

The final sprocket is an ANSI 8 tooth bike sprocket compatible with a standard bike chain. It was determined that this sprocket would lie approximately 3 feet from the tracking axis. Appropriately, a curved, U-shaped section of stainless steel was bent to a radius of 3 feet within which a section of bike chain was welded at both ends. This effectively created a large gear to be attached to the tracking axis and move synchronous with the earth's rotation.



Figure 4.5: Final Sprocket Orientation

Figure 4.5 shows the 8 tooth sprocket and bike chain assembly. A list of gears and their projected speeds, beginning with the bike chain, are listed in Table 4.1.

Table 4.1: List of Gears and Speeds

<b>Gear</b>	<b>Speed (rev/day)</b>	<b>Speed (rev/m)</b>
Bike Chain	1	0.016666667
8 Tooth Sprocket	40.6	0.676666667
102 Tooth Sprocket	40.6	0.676666667
6 Tooth Pinwheel	690	11.5
48 Tooth Sprocket	690	11.5

The structure design was initiated by fabricating the steel stand to properly fix the tracking axis above the eventual location of the reflector. This was done by cutting sections of 2” square tube steel, with 1/8” walls, to length and joining them with flat steel brackets using nuts and bolts so the stand could be disassembled and transported. A series of threaded shafts, bearings, tube steel and angle iron were used to construct the tracking arm on which the reflector would rest. Seasonal adjustment brackets were included which allow the angle of the reflector to be changed by moving a pin. The completed stand and gear system are shown holding the reflector in Figure 4.6.



Figure 4.6: Completed Tracking Stand

## CHAPTER 5

### ANALYSIS

#### 5.1: Energy Transmitted by Dish

The goal of this chapter is to show a step-by-step analysis of how the system should behave in Rajasthan. The first step in this process is an examination of the radiative energy being relayed from the sun to the thermal storage unit using the Scheffler dish. The energy from the sun ( $Q_{sun}$ ) is represented in Equation 5.1 in terms of the solar flux ( $q$ ), area of the dish ( $A$ ) and effective sun angle ( $\theta_{eff}$ ) for a given day.

$$Q_{sun} = qA\cos\theta_{eff} \quad (5.1)$$

In order to properly calculate this value, the solar flux and effective sun angle need to be investigated. The effective sun angle is dependent on the sun angle relative to the point of collection ( $\theta_{sun}$ ) and the tilt of the dish ( $\theta_{dish}$ ) (Equation 5.2).

$$\theta_{eff} = \theta_{sun} - \theta_{dish} \quad (5.2)$$

Both of these values change every 24 hours with the tilt of the dish being dependent on the relative sun angle. This relationship was investigated using 3D modeling software. Ideally, the shape of the dish would change with the sun angle, as discussed in Section 2.2, however, a dish design involving shape-change would not be cost-effective and would require advanced manufacturing techniques. Thus, the ideal dish shapes at the summer and winter solstices were generated and mapped against the curve of the dish at the equinox. The equinox curve was then pivoted until it most closely matched the ideal curves. This investigation is illustrated in Figure 5.1.

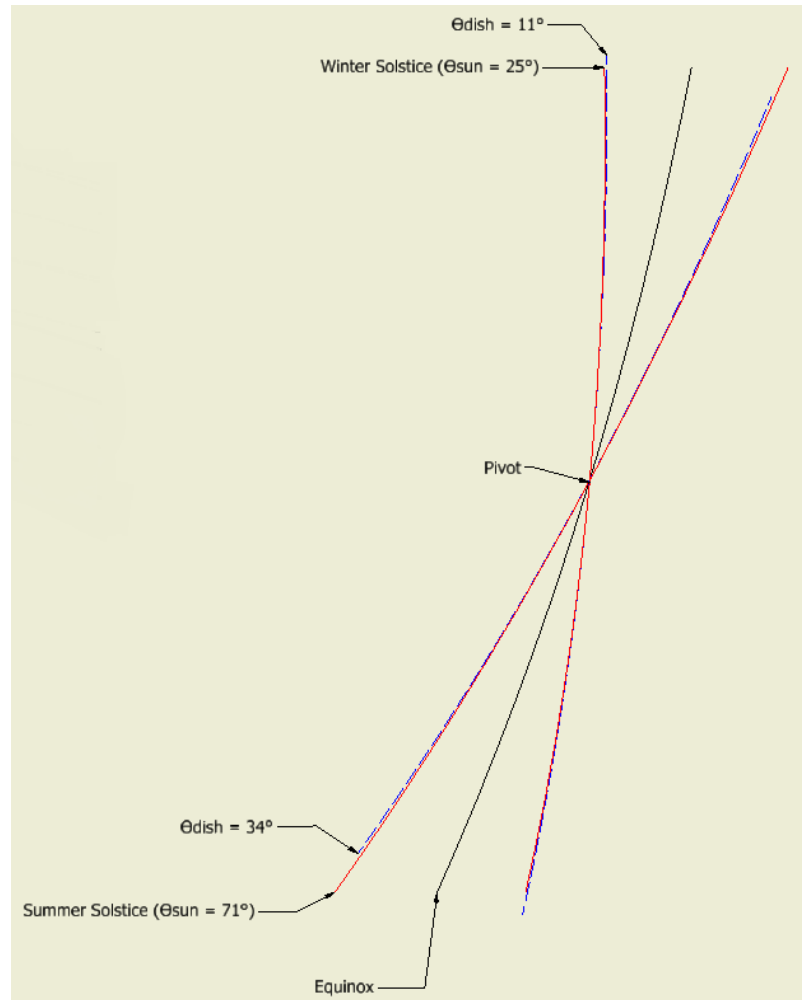


Figure 5.1: Dish Rotation vs. Ideal Design

The dish needs to be rotated  $11.5^\circ$ , half of the difference in sun angle ( $23^\circ$ ), in each direction to nearly match the ideal curve at each solstice. The dish design at the equinox has a tilt of  $22.5^\circ$ , so the  $\theta_{\text{dish}}$  values at the summer and winter solstices would be  $34^\circ$  and  $11^\circ$ , respectively. Though the curves are almost identical, the small deformation of curvature will still cause the focal spot to grow. Ray tracing software would be needed to more accurately investigate the effects of dish tilting on focal spot size, however, for the rest of this calculation it will be assumed that the storage unit is receiving energy from

the entire focal spot, regardless of season.

Now, because  $\theta_{\text{dish}}$  and  $\theta_{\text{sun}}$  values have been established,  $\theta_{\text{eff}}$  can be calculated at the equinox and solstices for Iowa and Rajasthan (Table 5.1).

Table 5.1: Equinox and Solstice Values for  $\theta_{\text{eff}}$

Region	Season	$\theta_{\text{sun}}$	$\theta_{\text{dish}}$	$\theta_{\text{eff}}$
Iowa	Equinox	48°	22.5°	25.5°
	Summer Solstice	71°	34°	37°
	Winter Solstice	25°	11°	14°
Rajasthan	Equinox	65°	25.25°	39.75°
	Summer Solstice	88°	36.75°	51.25°
	Winter Solstice	42°	13.75°	28.25°

The values for  $\theta_{\text{sun}}$  and  $\theta_{\text{dish}}$ , and therefore  $\theta_{\text{eff}}$ , vary linearly between solstices. Thus, a different value for  $\theta_{\text{eff}}$  is used every day to calculate the potential solar energy from the dish.

While the effective sun angle can be quite accurately calculated, the solar flux entering the system is dependent on the environment in which the dish is positioned and must be estimated based on scientific data. The solar energy flux per day (9 hour collection period) for Iowa and Rajasthan was estimated for each month using NREL data for each region (Figure 5.2). Iowa, like much of the United States, experiences a maximum solar energy flux in the summer and a minimum in the winter. India experiences a monsoon season that drastically reduces the solar energy available from June to August, giving it a pattern opposite to Iowa. The remaining months in India (September – May), however, experience solar fluxes greater than or equal to the summer months in Iowa.

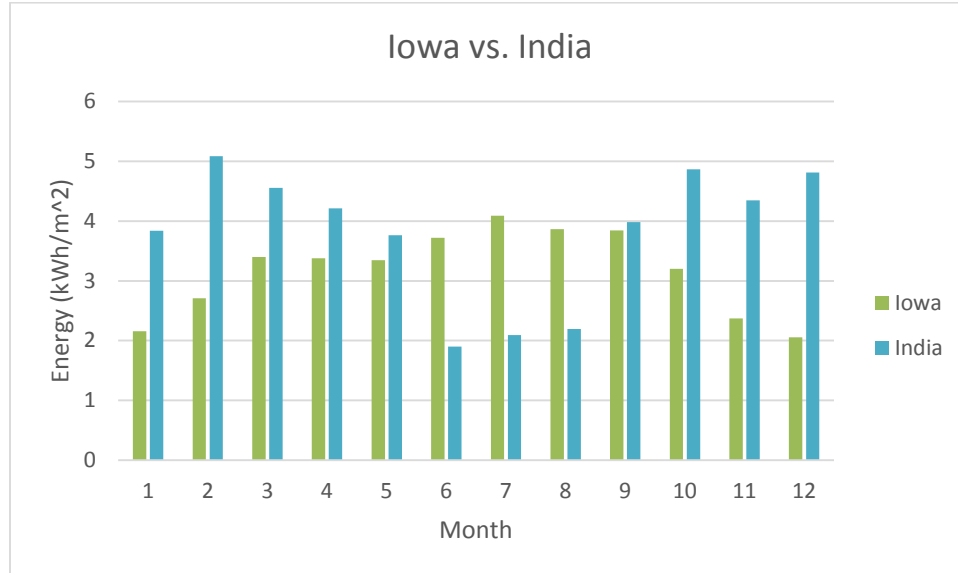


Figure 5.2: Solar Energy Flux for Iowa and India

For a dish with area ( $A$ ), the energy to the thermal storage unit, without losses, can be calculated for any day of the year. This calculation was done, in monthly intervals, for the designed system ( $A = 3 \text{ m}^2$ ) using data for Iowa and India. The results were used to generate third order polynomials that describe the energy into the storage unit during a 9 hour collection period: 7 a.m. to 4 p.m. in Iowa and 8 a.m. to 5 p.m. in Rajasthan (Table 5.2). These polynomials allow for subsequent calculations involving the behavior of the system throughout a collection period. The residuals corresponding to each polynomial are shown in Figures 5.3 and 5.4.



Table 5.2: Energy Polynomials

Month	Q(t) (Iowa)	Q(t) (Rajasthan)
January	$-0.0013t^3 + 0.0206t^2 + 0.1608t - 0.0009$	$-0.0103t^3 + 0.1422t^2 + 0.8102t + 0.001$
February	$-0.0007t^3 + 0.0134t^2 + 0.2367t + 0.0008$	$-0.0166t^3 + 0.2298t^2 + 0.9753t - 0.0296$
March	$-0.0018t^3 + 0.0274t^2 + 0.2786t + 0.0064$	$-0.0126t^3 + 0.1602t^2 + 1.102t - 0.0492$
April	$-0.0017t^3 + 0.0203t^2 + 0.3286t + 0.0024$	$-0.0113t^3 + 0.1533t^2 + 0.9439t - 0.0274$
May	$-0.0016t^3 + 0.0186t^2 + 0.331t - 0.0004$	$-0.0192t^3 + 0.2697t^2 + 0.4157t - 0.0274$
June	$-0.0016t^3 + 0.0183t^2 + 0.3781t - 0.0016$	$-0.0088t^3 + 0.1137t^2 + 0.3238t - 0.0022$
July	$-0.0015t^3 + 0.0184t^2 + 0.4118t - 0.0002$	$-0.009t^3 + 0.1184t^2 + 0.3612t - 0.0253$
August	$-0.0013t^3 + 0.0171t^2 + 0.3853t - 0.0023$	$-0.0063t^3 + 0.0798t^2 + 0.5248t + 0.0144$
September	$-0.0022t^3 + 0.0265t^2 + 0.3701t + 0.0035$	$-0.0066t^3 + 0.0697t^2 + 1.2401t - 0.0253$
October	$-0.0031t^3 + 0.0353t^2 + 0.2907t - 0.0006$	$-0.015t^3 + 0.1797t^2 + 1.2265t - 0.0014$
November	$-0.0039t^3 + 0.0474t^2 + 0.1571t + 0.0046$	$-0.02t^3 + 0.2563t^2 + 0.7624t - 0.014$
December	$-0.0024t^3 + 0.0337t^2 + 0.1243t + 0.0083$	$-0.0169t^3 + 0.2222t^2 + 0.9779t - 0.0253$

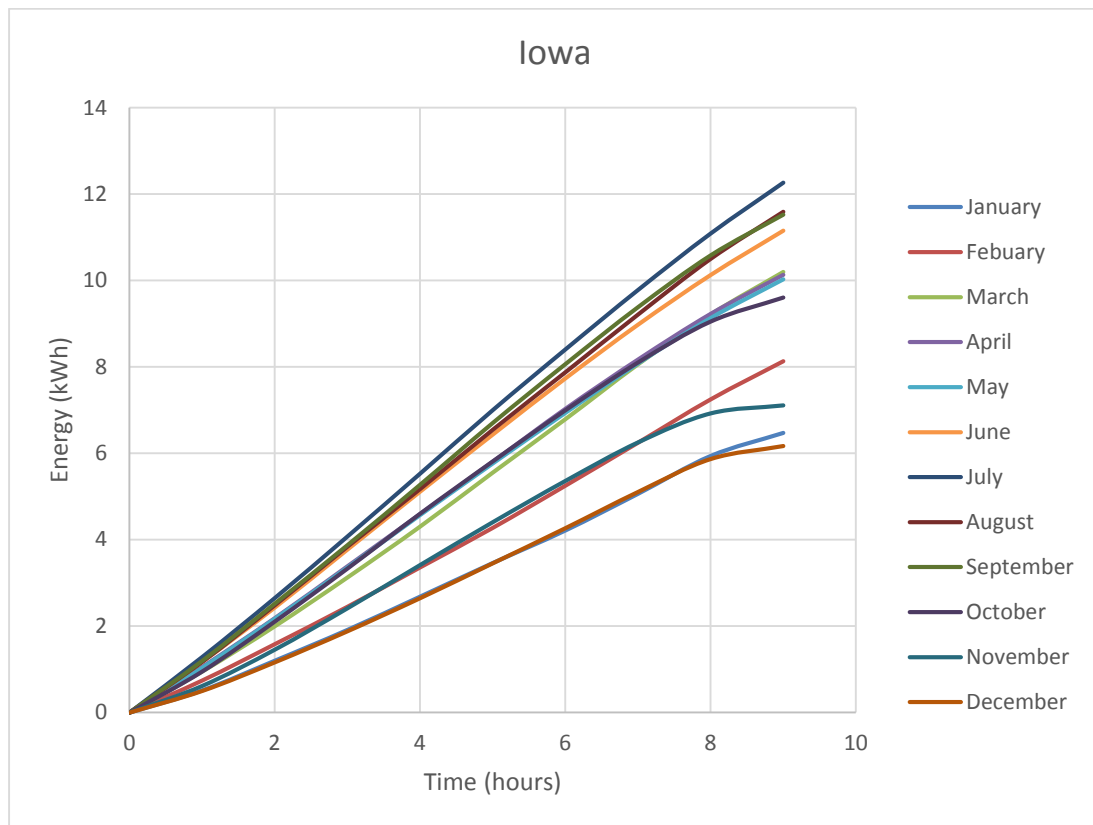


Figure 5.3: Monthly Iowa Energy Curves

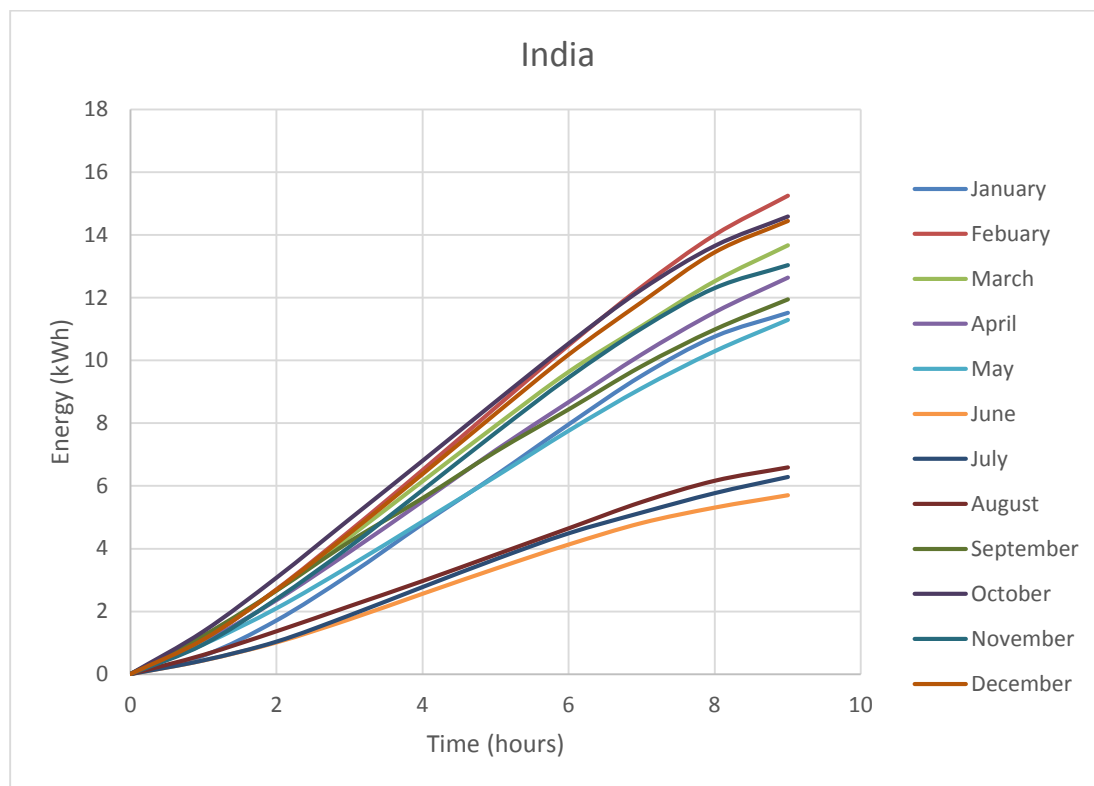


Figure 5.4: Monthly India Energy Curves

## 5.2: Testing

In the summer of 2014, upon the completion of the fabrication of the Scheffler reflector, testing was done to examine the temperature of the focal point. The first analysis of the reflector involved application of the focal point to some common materials. Wood, water and aluminum were among the materials tested in open-air tests in June. Upon application of the focal point, wood burned in approximately 3 seconds, water boiled in 1 minute and small chunks of aluminum began melting at around 5 minutes. A typical melting point of aluminum is 660 °C, showing that the reflector was performing quite well.

With this in mind, a second test was developed involving large samples of 4140 alloy steel. The samples were cut to lengths of 2.5 inches (0.0635 m) from a 3 inch (0.0762 m) diameter solid bar and had masses, on average, of 2.356 kg. Two holes were drilled in each sample for thermocouple positioning. The first hole was drilled through the center of the sample, from the rear, 2.375 inches deep, so the thermocouple would detect an approximate surface temperature. The second hole was drilled 0.25 inches deep, also from the rear, to determine the temperature change through the length of the sample. A sample was then placed in an aluminum sleeve, wrapped in high heat pipe insulation and inserted into a Styrofoam insulation box. Temperature data was gathered using a lap-top equipped with LabVIEW software and a DAQ card while converging the focal point on the sample. Figure 5.5 shows the experimental set-up.



Figure 5.5: Experimental Set-up

The first experiment, shown in Figure 5.6, along with a calculation of the Biot number (Equation 5.1), was used to prove that a lumped capacitance model could be assumed for the steel samples ( $Bi \ll 1$ ).

$$Bi = \frac{hL_c}{k} \quad (5.1)$$

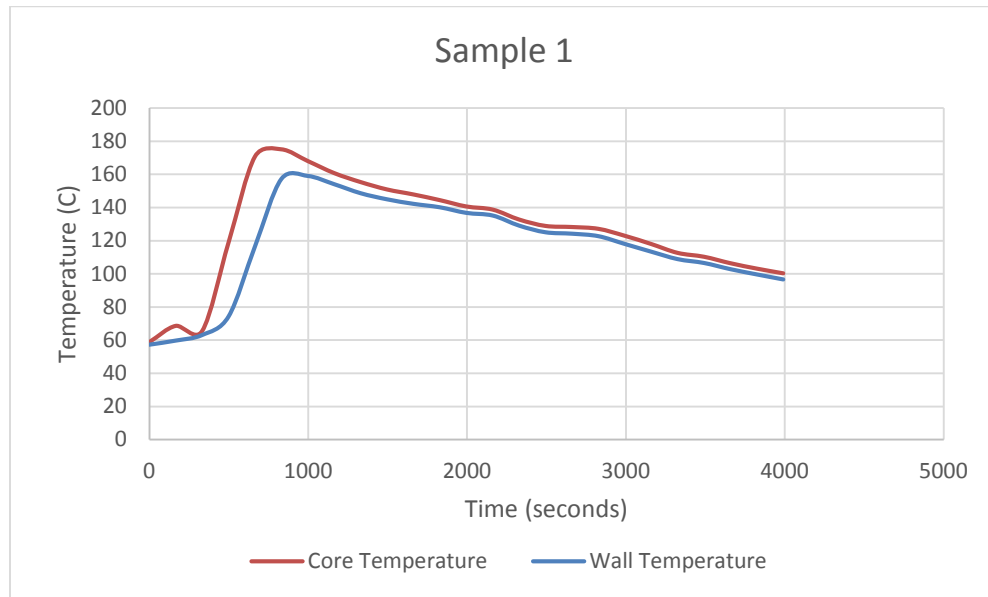


Figure 5.6: Heating and Cooling of Steel Sample

With the 4140 steel having thermal properties  $k = 42.7 \text{ W/m-K}$ ,  $h = 150 \text{ W/m}^2\text{-K}$  and a characteristic length of  $0.0635 \text{ m}$ , the Biot number was calculated as  $0.223$ . The experimental data, supported by the calculation, shows that the temperature change through the sample is minimal, hence, energy losses within the sample can be neglected. The energy balance of the sample can now be represented in terms of temperature change of the sample, energy into the sample, conductive losses and convective losses (Equation 5.2).

$$mc_p(T - T_\infty) = Q_{sun}\alpha R - \frac{kA_s\Delta t}{L}(T - T_\infty) - h_{air}A_f\Delta t(T - T_\infty) \quad (5.2)$$

The rear thermocouple was removed and a new sample was heated for a longer time period. Equation 5.2 was then used to investigate the effects of dish reflectivity ( $R$ ) and sample absorptivity ( $\alpha$ ) on the efficiency of the system. The values used to evaluate Equation 5.2 are given in Table 5.3. The area of the face exposed to the air is represented as  $A_f$  while  $A_s$  is the remaining surface area (covered by insulation). The energy entering the system,  $Q_{\text{sun}}$ , was found by integrating the Iowa polynomial for July between the times of 2:00 ( $t = 6$ ) and 2:30 p.m. ( $t = 6.5$ ); the approximate times at which energy was entering the system. The residuals from the second experiment and the approximate behavior of the sample in the absence of clouds are shown in Figure 5.7.

Table 5.3: Values for Steel Sample Energy Balance

System	
$Q_{\text{sun}}$ (kWh)	0.316
$T$ (C)	500.5
$T_{\infty}$ (C)	17.3
$\Delta t$ (hours)	0.495
$h_{\text{air}}$ (kW/m <sup>2</sup> -K)	0.008
Sample	
$m$ (kg)	2.356
$c_p$ (kWh/kg-K)	0.000137
$A_f$ (m <sup>2</sup> )	0.0182
$A_s$ (m <sup>2</sup> )	0.0486
Insulation	
$k$ (kW/m-K)	0.00003
$L$ (m)	0.152

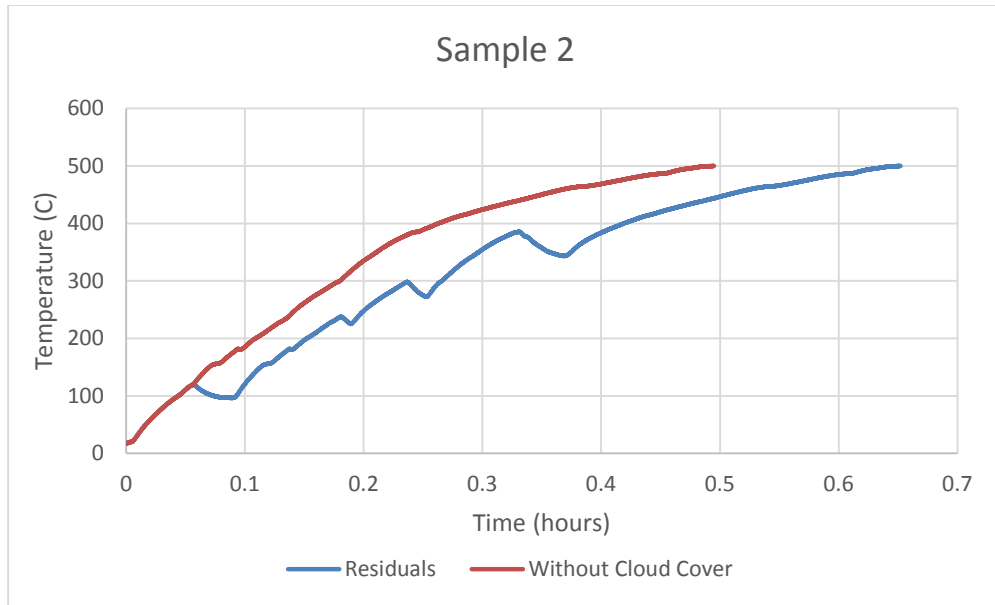


Figure 5.7: Heating of Second Steel Sample

The overall energy into the system was estimated to be 0.230 kWh. The actual energy stored by the system was 0.156 kWh. After including losses due to conduction and convection the absorptivity and reflectivity, efficiencies were calculated with a lumped value,  $\alpha R$ , of 0.841.

Though the calculation accounts for cloud cover, there are a few inconsistencies within the experiment that can alter the efficiency. For example, the focal spot was slightly larger than the absorption surface and the dish had to be manually adjusted. As a result, a small fraction of the energy from the dish was not transmitted to the sample. Also, it is likely that the solar energy on the day of testing did not exactly correspond with the polynomial representative of solar energy available in July. Furthermore, the durability of the Styrofoam made the sample vulnerable to extra convective losses, as the box began to melt halfway through testing due to high temperatures.

### 5.3: Thermal Storage Unit Analysis

The results from the investigations in Sections 5.1 and 5.2 were utilized for a bulk analysis for the thermal storage unit described in Section 3.3. The goal of the analysis was to describe the variation in storage unit temperature over a 72 hour period, broken into 24 hour intervals, when subjected to solar energy in Rajasthan using a similar Scheffler reflector. Table 5.4 describes the constraints of each 24 hour interval.

Table 5.4: System Energy Constraints

Interval (hours)	Constraint	Explanation
0 - 9	Heating	Appropriate Energy Polynomial
9 - 11	Cooking	Loss of 2 kWh
11 - 22	Dormant	Exposed to Conductive Losses
22 - 24	Cooking	Loss of 2 kWh

During the heating of the unit, conduction and convection are acting on the system and in its dormant stage (night), the absorption surface will be covered by insulation, resulting in only conductive losses.

A spreadsheet was designed to continuously evaluate Equation 5.2 for 24 hour intervals using a series of “if” statements. These statements were mainly used to describe the latent heat phase in which the solar salts melt and the temperature of the system stays constant at their melting temperature (220 °C). The current solar salt configuration for the storage unit, material properties and energy required for the latent heat phase are shown in Table 5.5.

Table 5.5: Properties of Latent Heat Phase [11]

Property	NaNO <sub>3</sub>	KNO <sub>3</sub>
Mass (kg)	14.1	9.4
Molar Mass (kg/mol)	0.101	0.085
Moles	139	111
Enthalpy of Fusion (kWh/mol)	0.00466	0.00256
Average Enthalpy (kWh/mol)	0.0034	
Required Energy (kWh)	0.85	

Thus, the unit will heat until reaching 220 °C and then need to absorb 0.85 kWh of energy before continuing to rise in temperature. The other specifications of the system, used in Equation 5.2, are given in Table 5.6.

Table 5.6: Storage Unit Specifications

Storage Unit	
m (kg)	35.75
$c_p$ (kWh/kg-K)	0.00025
Energy Into System	
$Q_{\text{sun}}$ (kWh)	$Q(t)$
$\alpha$	0.75
R	0.9
Conductive Losses (rice hulls)	
k (kWh/m-K)	0.00005
$A_s$ (m <sup>2</sup> )	0.365
L (m)	0.4572
Convective Losses (air)	
h (kWh/m <sup>2</sup> -K)	0.008
$A_f$ (m <sup>2</sup> )	0.073
$T_\infty$ (C)	25

A few assumptions were made to simplify the calculation. The acrylic mirrors used on the reflector were assumed to have a reflectivity of 0.9. If the value from Section 5.2 for  $\alpha R$  were used for this calculation the value of  $\alpha$  would be 0.934. However, because of uncertainty in the accuracy of the experiment, a more conservative value was



assigned for  $\alpha$  (0.75). Again, to simulate a single temperature for the model, lumped capacitance was assumed for the calculation.

The calculation of the temperature of the system was done in multiple steps.

First, the temperature ( $T_{ref}$ ) was found for an ideal system using Equation 5.3 (Equation 5.2 with no losses).

$$mc_p(T_{ref} - T_\infty) = Q_{sun}\alpha R \quad (5.3)$$

Then, the temperature ( $T_2$ ), for the system with losses, was found using Equation 5.4 (Equation 5.2 using  $T_{ref}$  to calculate the losses).

$$mc_p(T_2 - T_1) = Q_{sun}\alpha R - \frac{kA_s\Delta t}{L}(T_{ref} - T_\infty) - h_{air}A_f\Delta t(T_{ref} - T_\infty) \quad (5.4)$$

This process was iterated every 0.1 hours to produce Figure 5.8 for polynomials,  $Q(t)$ , from February and August in India, the months with the highest and lowest available solar energy, respectively.

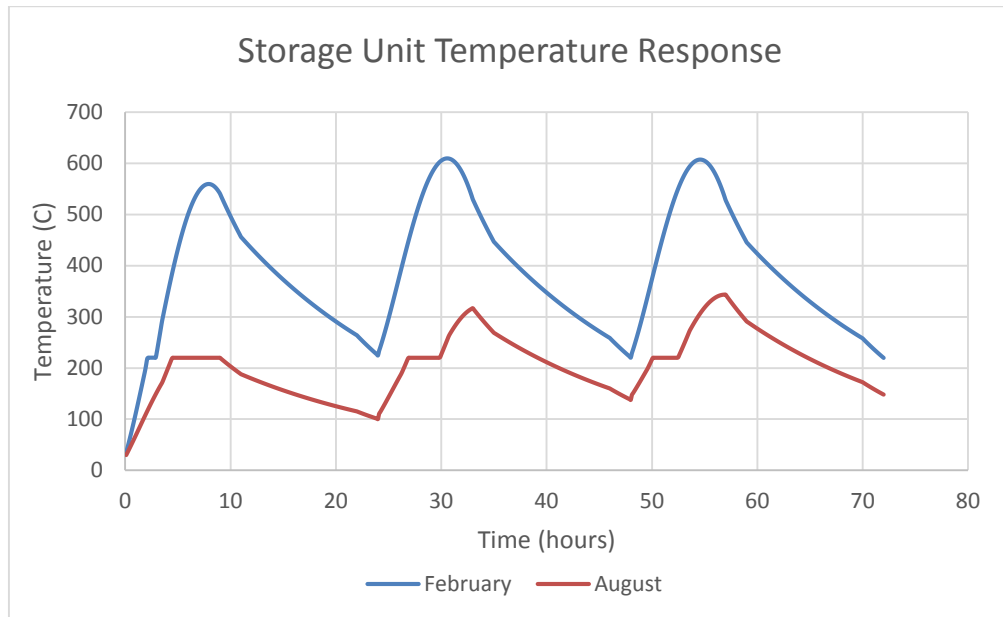


Figure 5.8: Thermal Storage Unit Temperature Response

The results presented in Figure 5.8 are encouraging when compared to past calculations and experimental data. A clear comparison can be made between Figure 5.8 and the simulations by Ruebush, presented in Section 3.2. The maximum temperatures experienced in the Ruebush simulations are relatively close to the maximum temperature in the February calculation. Comparisons can also be made in relation to the second experiment in Iowa (Figure 5.7). The maximum temperature in the experiment was approximately 500 °C during a month in which the average daily energy into the system was 10.2 kWh. The average energy into the system in India, in February, is 15.2 kWh, resulting in a maximum temperature of about 600 °C, via the calculation. Although a perfect correlation is not present, it is clear that the calculation, given the lack of experimental data for the entire system for comparison, is a good representation of how the thermal storage unit would behave in India.

Many derivations of the calculation can be simulated to investigate the effects of physical changes to the system. If temperatures of 600 °C were reached using the existing prototype it is possible the aluminum core could melt. Appropriately, for the month of February, in India, some aspects of the system were fluctuated to show the effects on storage unit temperature. Figure 5.9 shows the storage unit temperature with varying reflector areas. A reduction in reflector area results in a decrease in maximum temperature and shrinks the range of temperatures experienced throughout the entire simulation. A reflector with an area of 1.5 m<sup>2</sup> experiences maximum temperatures around 400 °C and reasonable morning cooking temperatures just below 200 °C. Thus, upon comparison with the August curve from Figure 5.8, a dish of area 3 m<sup>2</sup> could be used during the months with low solar energy and then partially covered in higher energy

months to produce appropriate storage unit temperatures.

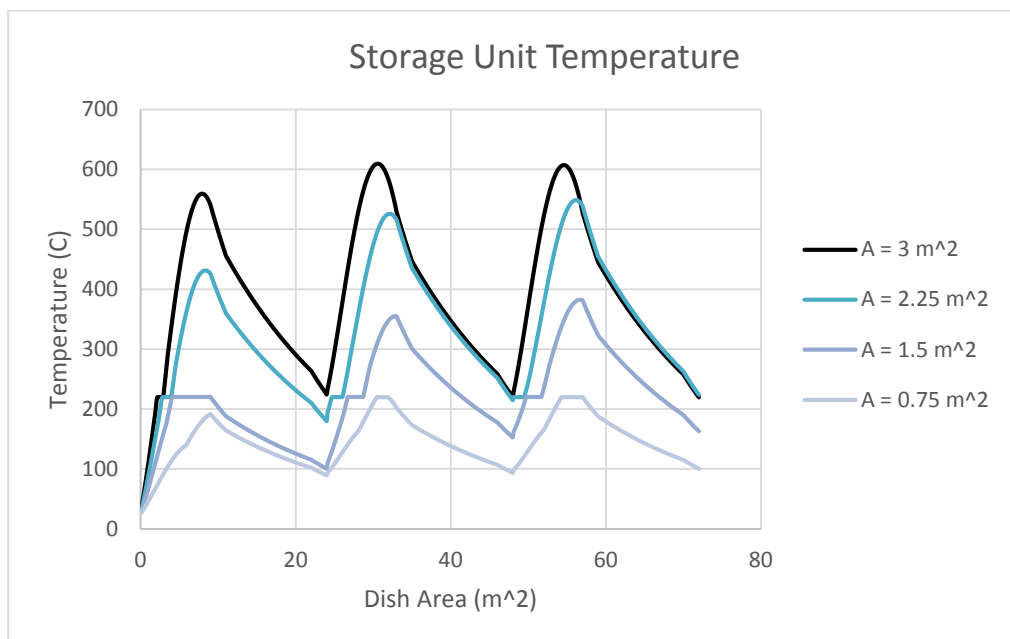


Figure 5.9: Storage Unit Temperature by Reflector Area

Another investigation was performed to observe the temperature change when extra solar salts were added to the system (Figure 5.10).

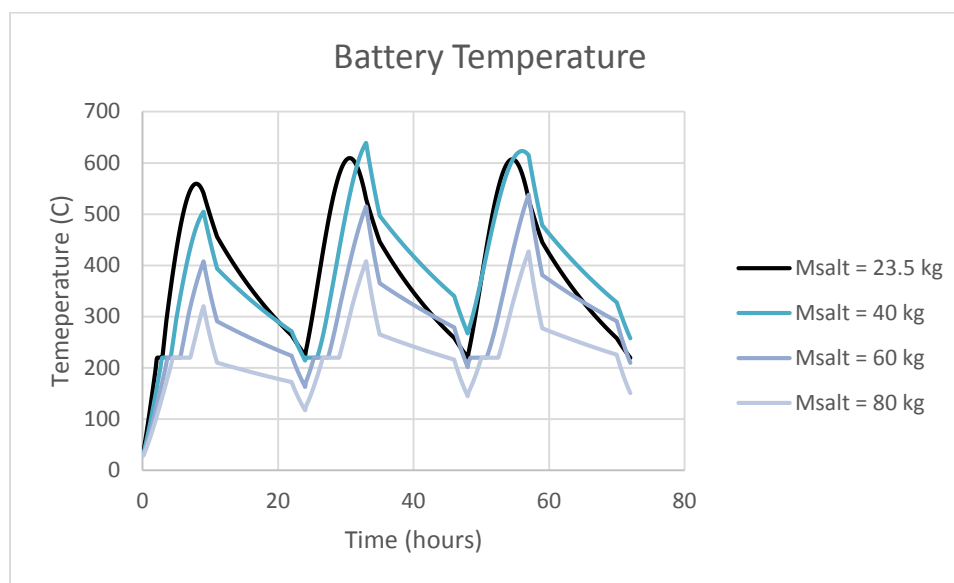


Figure 5.10: Storage Unit Temperature by Mass of Solar Salts

When mass is added to the system, the heat capacity is raised as well as the energy required to melt all of the salts, resulting in longer latent heat phases and less losses.

However, to bring the temperatures down to a reasonable range, the weight of the system would have to be nearly tripled. Therefore, there is no immediate need for additional salt in the storage unit.

## CHAPTER 6

### CONCLUSIONS

#### **6.1 Conclusions**

The research outlined in this thesis was completed to help achieve the goal of developing an affordable, thermal storage solar cooking system that can be used in developing countries. A Scheffler reflector, with a small and accurate focal point, was created along with a support stand equipped with tracking capabilities. These components were designed for integration with a thermal storage unit, for testing, but also to understand the complexities of producing a system that follows all of the design constraints outlined in Section 1.2.

Temperature data was collected using the Scheffler reflector and utilized to model the behavior of the storage unit. Inconsistencies exist within the model, however, it gives a general representation of how the storage unit should behave, in terms of temperature, and provides a summary of the elements of heat transfer present in the system.

Overall, the efforts made in this research were not aimed toward producing a system usable in India but to take steps in the direction of that goal by advancing the understanding of the work required to produce such a system.

## 6.2 Recommendations

In order to further investigate the effectiveness of this prototype, a few things must be accomplished. First, the response of the thermal storage unit must be examined when heated with the Scheffler reflector. The data collected could then be compared to the calculations from Chapter 5.

Next, the tracking system must be equipped with technology capable of moving the reflector for an extended period of time. A pendulum was never attached to the gear system due to deficiencies in time, man power and practicality in relation to data collection. An electrical component, perhaps a stepper motor, could be easily integrated with the system and would allow for hours of testing to be done with minimal work to be done by the user.

Lastly, the entire prototype could be operated as it is intended. Extensive work would be needed involving the implementation of a pendulum and counterweight system. Then, an overall feasibility study would be possible involving a system design optimization. There are many things to consider: a cost-effective way to manufacture a lighter Scheffler reflector, reducing the amount of materials used in construction of the stand, manufacturing capabilities in India, alternative reflective materials, etc.

## 6.3 Future Work

Work in this area at the University of Iowa is continued by Mike Augspurger (referenced in Section 3.3). He is developing a computational model to simulate the

temperature behavior within the thermal storage unit. Figures 6.1 and 6.2 show two of the simulations that he has completed. The temperature of the salts can be observed, in Figure 6.1, after a small time interval when heat is applied to the exposed aluminum face (right side). The approximate shape of the aluminum core is shown by the outline. Figure 6.2 shows the temperature distribution, after a longer time interval, in the salts as well as within the core.

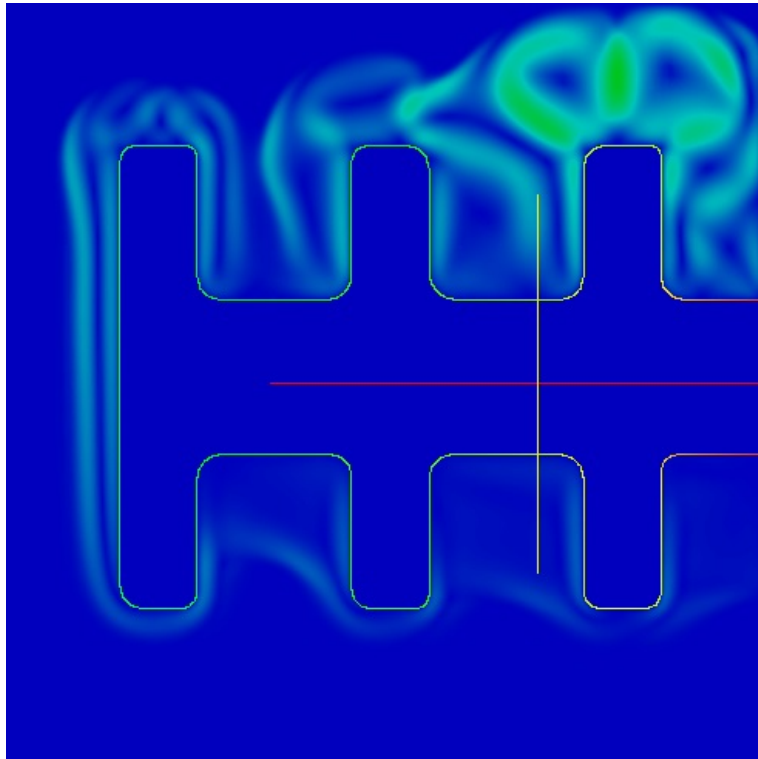


Figure 6.1: Low Heat Solar Salt Temperature Distribution

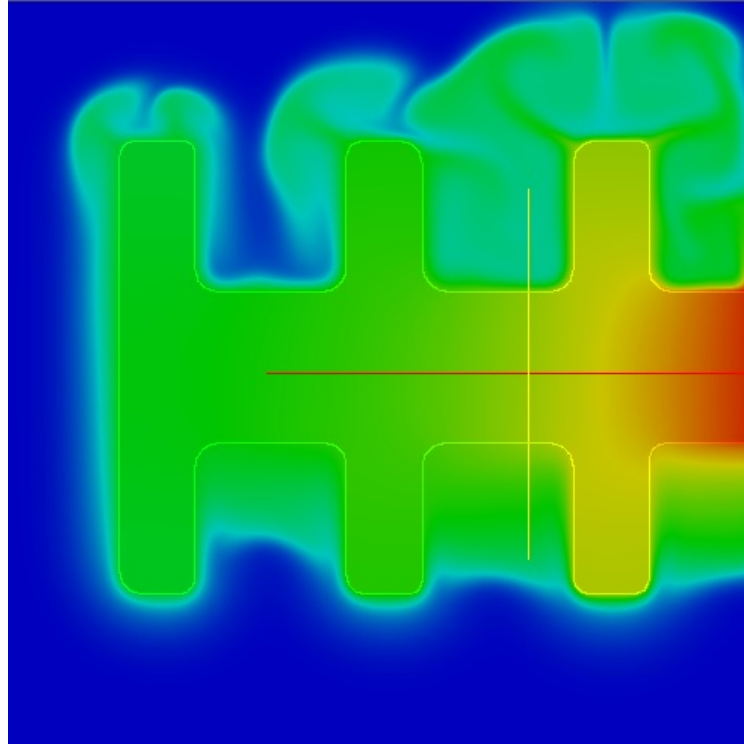


Figure 6.2: Overall Storage Unit Temperature Distribution

Further modifications to the core design within the computational model, along with experimental data, will allow for a redesign of the storage unit resulting in more efficient heat transfer within the system.



## REFERENCES

- [1] Energy For Cooking in Developing Countries. (2006). In *World Energy Outlook 2006* (2nd ed., Vol. 1, pp. 419 - 445). Paris, France: IEA.
- [2] Akinwale, P. (2006). Abstract. In *Development of an Asynchronous Solar-Powered Cooker* (p. 2). Massachusetts Institute of Technology.
- [3] Valmiki, M., Li, P., Heyer, J., Morgan, M., Albinali, A., Alhamidi, K., & Wagoner, J. (2010). A Novel Application of a Fresnel Lens for a Solar Stove and Solar Heating. *Renewable Energy*, 36, 1164-1620.
- [4] Rapp, J., & Schwartz, P. (2010). *Construction and Improvement of a Scheffler Reflector and Thermal Storage Device* (pp. 1164 - 1620). Cal Poly Physics.
- [5] Munir, A., Hensel, O., & Scheffler, W. (2010). Design principle and calculations of a Scheffler fixed focus concentrator for medium temperature applications. *ScienceDirect*, 84, 1490-1502.
- [6] Scheffler, W. (n.d.). *INTRODUCTION TO THE REVOLUTIONARY DESIGN OF SCHEFFLER REFLECTORS* (pp. 1 - 4). Aislingen, Germany.
- [7] National Solar Radiation Data Base. (n.d.). Retrieved September 5, 2014, from [http://rredc.nrel.gov/solar/old\\_data/nsrdb/1991-2010/hourly/list\\_by\\_state.html](http://rredc.nrel.gov/solar/old_data/nsrdb/1991-2010/hourly/list_by_state.html)
- [8] Updated India Solar Resource Maps. (n.d.). Retrieved October 3, 2014, from [http://www.nrel.gov/international/ra\\_india.html](http://www.nrel.gov/international/ra_india.html)
- [9] Ruebush, S. (2013). Simulation Results. In *A COMPUTATIONAL STUDY OF THERMAL STORAGE TECHNIQUES FOR SOLAR COOKING DEVICES FOR USE IN RAJASTHAN, INDIA* (pp. 1 - 55). University of Iowa.
- [10] Augspurger, M. (2013). *Testing a Prototype for a Solar-Powered Thermal Bank* (pp. 1 - 14). University of Iowa.
- [11] Cordaro, J., Kruienza, A., Altmaier, R., Sampson, M., & Nissen, A. (n.d.). *THERMODYNAMIC PROPERTIES OF MOLTEN NITRATE SALTS* (pp. 1 - 8). Livermore, California: Sandia National Laboratories.